

# ALMA Memo 599

## The ALMA Calibrator Database I: Measurements taken during the commissioning phase of ALMA

T.A. van Kempen<sup>1,2</sup>, R. Kneissl<sup>1</sup>, N. Marcelino<sup>3</sup>, E.B. Fomalont<sup>3,1</sup>, D. Barkats<sup>1</sup>, S.A. Corder<sup>1,3</sup>, R. Lucas<sup>1,4</sup>, A. B. Peck<sup>1,3</sup>, and R. Hills<sup>1,5</sup>

<sup>1</sup>Joint ALMA Observatory (JAO), Alonso de Córdova 3107, Vitacura, Santiago, Chile

<sup>2</sup>Allegro ARC node, Leiden Observatory, Niels Bohrweg 2, Leiden, the Netherlands\*

<sup>3</sup>National Radio Astronomy Observatory, (NRAO), 520 Edgemont Road,  
Charlottesville, VA, USA

<sup>4</sup>Institut de Planétologie et d'Astrophysique de Grenoble (IPAG), 414 Rue de la Piscine,  
St-Martin d'Hères, France

<sup>5</sup>Cavendish Laboratory, 19 JJ Thomson Ave, Cambridge CB3 0HE, United Kingdom

Submitted: December 2, 2014

### Abstract

Interferometric ALMA observations rely upon accurate and trustworthy calibration of the instrumental and atmospheric phase and amplitude variations in order to produce high quality scientific data. Short observations (scans) of radio sources at the appropriate cadences are included in observing programs in order to determine these variations with time and frequency. Quasars are among the best radio source candidates because their emission is bright, lack spectral features and are point-like; typically they measure less than 0.01'' in size. Since quasar flux densities vary both in time and frequency, specialized ALMA observations are needed to find the quasars that are sufficiently bright between 90 and 900 GHz, the ALMA frequency range. Once found, the appropriate quasar flux densities must be monitored with periodic ALMA observations to track. Hence, in 2011, the ALMA calibrator database was initiated during the commissioning and science verification stage of ALMA. This memo describes the database structure and contents, the observational and data reduction strategy, and discusses many properties of the radio sources observed to this date. During the commissioning phase, two major observing programs were started: First, a *wide* survey of about 600 quasars was carried out with the aim to obtain a sufficiently large sample of sources to be used as phase reference sources. Second, a selection of about 45 bright and relatively stable quasars, called *grid* sources, were monitored regularly. The sample was distributed relatively equally over the sky. These are candidates for bandpass calibrations, but have since also evolved into secondary amplitude calibrator candidates. Both programs have continued into the operational phase of ALMA.

---

\*contact e-mail: kempen at strw.leidenuniv.nl

## Introduction

A radio wave in its path through to atmosphere above each antenna to the correlator varies in gain and phase (delay) over a variety of time-scales. The changes must be calibrated before ALMA can produce scientifically useful data, often in the form of images or spectral cubes. Gain and phase changes in the electronics generally have a time scale of many minutes to hours. Shorter-term variations are dominated by the atmospheric delay and absorption of the radio signal above each antenna, introduced by atmospheric turbulence.

Phase fluctuations at the shortest time-scales (<2 min) can be corrected using 181-185 GHz measurements from radiometers on each of the antennas. The fluctuations in the measured water vapor emission along the line of sight can be converted into delay changes of the incoming signal (See ALMA Memo 593, Nikolic et al., 2012).

The variations on timescales between these two cases (~4 min to half an hour) can be calibrated by switching observations between a nearby calibrator and the science target.

Quasi-stellar objects (often referred to as QSO's or quasars) provide the majority of calibrator radio sources because they are bright at radio wavelengths and have point-like emission. Quasars are found in all regions in the sky and are observable through the Galactic disk. Essentially, quasars provide "test" signals relatively close in the sky to the scientific target. When observations are alternated between the two, any changes in the gain and phase of the quasar signals are transferable to the target data, largely removing variations introduced by the atmosphere. As such, it is essential to obtain the parameters of quasars across the sky before carrying out the scientific observations.

At radio frequencies below 20 GHz the spectral index,  $\alpha$  where flux  $\propto \nu^\alpha$ , lies between +0.5 to -0.7. At the typical ALMA frequency of 300 GHz, the spectral index is more constrained, ranging from -0.2 to -1.0. The emission mechanism is synchrotron and the spectral index is associated with the power distribution of the radiating electrons and with the optical depth in regions of the radio source. Planck results revealed another clear difference between the spectral slope from 300 GHz and that above 1000 GHz (Planck Collaboration et al., 2011a), likely caused by the increase in thermal emission at higher frequencies. For a good discussion on the nature of spectral slopes at high radio frequencies as well as the most recent observational evidence, see Planck Collaboration et al. (2011b,a, 2013).

Due to intrinsic physical changes of quasar, observed flux densities vary in time and frequency. Typical flux density changes are about 10% over a month. However, some quasars exhibit much larger changes, perhaps by a factor of two or three over a month or two. In a handful of quasars changes of an order of magnitude have been observed. Changes of up to 5% on a daily basis are also known. Quasar emission does not show periodic changes, and the most extremely variable quasars tend to stay very variable for many years. At the ALMA resolution of 0.1", the variable quasar flux densities remain point-like, because the emission changes occur within a region of about 0.005" of the nucleus.

The use of quasars as calibrator sources has motivated other radio observations over the decades to carry out monitoring programs which are contained in catalogs, many of which are publicly available. Examples are the OVRO (Richards et al., 2011), AT20 (Massardi et al., 2011), VLA (Patnaik et al., 1992), VLBA (Beasley et al., 2002; Fomalont et al., 2003), SMA (Gurwell et al., 2007) and recent Planck catalogs (Planck Collaboration et al., 2011b,a, 2013). One of the oldest quasar catalogs is the Third Cambridge Catalog (Edge et al., 1959). Due to the available southern declinations at ALMA, the AT20G (Massardi et al., 2011) is particularly interesting, and contains many potential ALMA calibrators.

Since ALMA observes at a much higher frequency than is available from most of the above catalogs, excepting the extensive catalogs of the SMA and PdB <sup>1</sup> (Gurwell et al., 2007), but both located on the northern hemisphere, there was strong motivation to start an ALMA monitoring program and database construction suitable for (sub)millimeter calibration. It was also important to measure the spectral index of these sources in order to estimate their flux densities at frequencies over the entire ALMA frequency range, in particular to frequencies above 300 GHz where little to no information exists.

The first part of this memo describes the ALMA's calibrator database. It then outlines the two main observing programs: 1) the database filling of quasars over as much of the observable sky as possible, 2) the observations and monitoring of about 45 bright and/or stable quasars at 95 and 350 GHz. Fainter quasars can be used as phase references of science targets, while the brighter sample are used for more stable bandpass calibrations, especially those where strong signals are needed in narrow-band channels.

---

<sup>1</sup> see e.g. <http://sma1.sma.hawaii.edu/callist/callist.html>

Figure 1: Screenshot of the web-based interface to the calibrator database. The first tab contains the query parameters.

## The ALMA calibrator database

In order to compile and have available information about quasar calibrators, a dedicated database system was designed. The ALMA calibrator database is a read/write database. It has the capability to both accept new entries and modify existing ones. Entries are denoted as measurements. Only ALMA staff members are able to enter and modify measurements.

As a reference, a list of over 5,000 calibrator candidates was made, filled mainly from low frequency catalogs (VLA, SMA, CRATES, AT20), with the CRATES compilation being the main contributor. The inclusion of the VLA catalog and the SMA catalog contributions are specifically aimed at higher frequencies. Since many of the sources were probably too weak to be useful even at 90 GHz, an ALMA observing database filling program began in 2011 to identify the suitably strong calibrators of this list. These observations are described in the next section. Another problem was the use of inaccurate positions for some of the sources in the catalog. To remedy this, VLBI-quality positions, often accurate to 0.001", from ICRF and related catalogs were substituted, where available. Finally many sources in the 20 GHz AT20g catalog were included to fill the southern sky (dec < -40°) with candidate sources. Note that few VLBI-quality positions were available in the southern sky.

Most catalog updates are now done using flux densities measured regularly with ALMA. Measurements of the degree and angle of the linear polarization have also started, and occasionally an improved source position is added. Nearly all of the quasars that are used are point sources with ALMA resolution, so that detailed structural information is not needed. A few sources with faint large-scale structure (e.g., 3c273) are noted in the catalog. Such sources are still good calibrators except at the very lowest resolutions. When ALMA begins higher resolution observations, the contribution of thermal emission, expected to be somewhat extended, more structure information and images will be provided.

The database is accessible through:  
<http://almascience.eso.org/sourcecatweb/search>

The query form is on the first tab, as shown in Fig. 1. By position, the database can be queried on Source name or coordinates. A radius in degrees can be given. In addition, constraints can be put in by energy, both in frequency and in flux density, as well as time, expressed by a start and end date. After query, the results are found in the second and third tabs, providing the numbers and a graphical representation (See Fig. 2 and 3

If a calibrator is designated in the Source name, then information about this source is given in the Result Table and the Result Plot. If a non-calibrator source is specified, then all ALMA catalog calibrators within the Search Radius will be listed in the Table and Plot.

Most calibrators do have several names. The official ALMA name designation has the form *JHHMM-DDMM* for all objects using the J2000 coordinate system. However, the catalog contains major aliases



Figure 2: Screenshot of the web-based interface to the calibrator database. The second tab provides the resulting sources produced by the query.

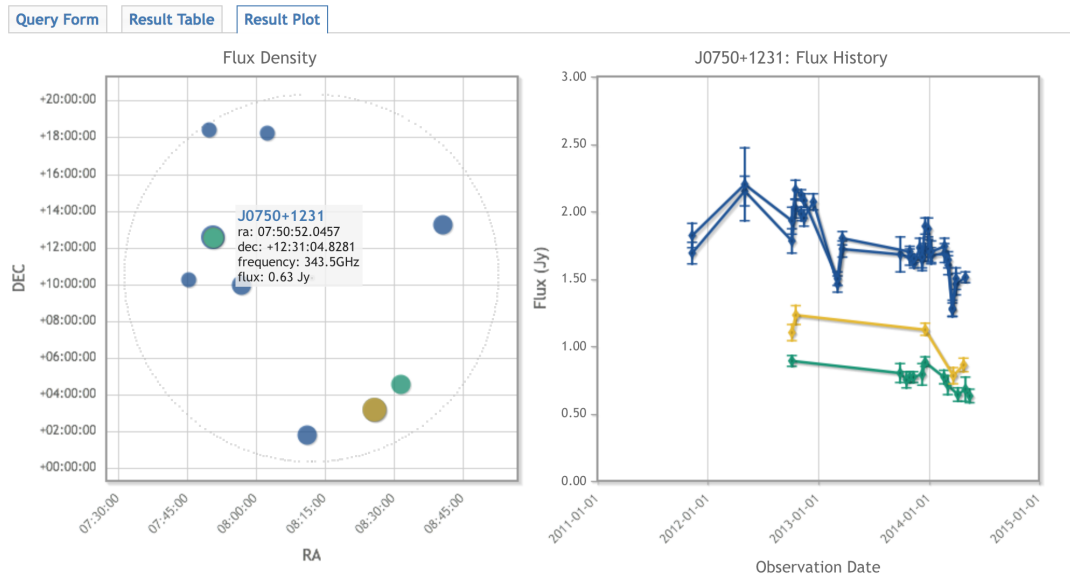


Figure 3: Screenshot of the web-based interface to the calibrator database. The third tab shows a graphical interface. To the left, results found within the defined radius are shown. If an individual source is selected, the flux density history is plotted to the right.

for all sources so selection by other common names is available. For example, the recognized names for J1229+0203 are: J1229+020, 3C273, 3c273, B1226+023. For J1325-4301: B1322-427, J1325-430, cena. It is advised to check alternative names. Some sources (e.g. Centaurus A as cena) are only included to be used as calibrators if certain controlled conditions are met.

After querying the database, results are provided in a table in the second tab. The table is produced with the source names, right ascension, declination, separation from the queried coordinates, observed frequency and its associated ALMA Band, flux density, flux density error uvmax, uvmin and the date at which this was obtained. This tab is available for download in CVS and JSON formats. The last tab shows the spatial distribution of calibrators around the provided location up to the chosen radius. The point size of the calibrators is scaled to the brightness, while the color shows the highest ALMA Band within the query definitions where a measurement exists. See Fig. 2 for an example. If a calibrator is selected, the flux density history of that source in all ALMA Bands defined during the query. If no constraints were put in, the flux density history of all ALMA Bands is plotted.

## Database Filling

For adequate calibrations of ALMA observations, at least two types of calibrators are needed. First, strong quasars are used to determine the bandpass (receiver response over the range of observed frequencies) of each antenna system. These do not need to be close to the science target, but are required to be as bright as possible at the targeted bandwidth and frequency. In practice, a sufficient number of these bright calibrators are needed so that at least one of them has elevation above about  $40^\circ$  at any sidereal time. A second sample of calibrators can be weaker but must be much more numerous in order to have a high probability of finding a suitable candidate close to any position in the sky, thus covering all potential science targets. Their strength needs to be sufficiently large to determine the amplitude and gain at each antenna to about 3% in gain or  $5^\circ$  in phase with about a one minute scan. Note that these requirements are slightly less strict at observations above 400 GHz.

The initial observations in determining these calibrators was started during the Commissioning and Science Verification (CSV) phase of ALMA. This work has continued during the science operations phase and will continue for many more years. Other calibrator types, for example polarization calibrators, will be defined and observed when needed.

## Grid Quasar sample

A candidate bright quasar sample was collected from previous catalogs (existing catalogs from the SMA, ATCA, VLA; Beasley et al. (2002); Gurwell et al. (2007); Massardi et al. (2011)), searching for those estimated to be stronger than 1 Jy at 100 GHz and a declination below  $+45^\circ$ . An assessment of their variability was also made. Note that some of these quasars are located at northern latitudes ( $\delta > 20^\circ$ ) and are thus only available for a brief time each day. The final list of 45 quasars was chosen to cover the sky relatively uniformly and includes those both with the most stable emission, as well as the strongest semi-regular flaring quasars. This set of sources was named the *Grid* sample, and is primarily aimed at bandpass calibrations where good signal-to-noise is needed for accurate narrow-channel receiver response calibration. The Grid sources were also extensively used for a large number of other commissioning tasks (e.g., receiver stability testing, pointing models, bandpass stability, etc).

The use of the Grid sample as secondary absolute flux density calibrators evolved over the 2011-2013 period because of the difficulty in using solar system objects (SSO). Although SSOs possess relatively accurate flux density models, a suitable SSO is often not available during an observations, or at a high frequency and resolution, all available SSOs are too resolved to calibrate longer baseline data. Thus, monitoring the grid sample on a semi-regular basis was initiated in order to estimate their flux density at any time and frequency to a 10% level.

The main goals of the monitoring were: (1) to quantify variability of the brightest quasars at various ALMA frequencies; (2) to identify the best candidates for bandpass calibrations; (3) to provide up to date flux densities necessary for commissioning and other start-up calibrations and (4) investigate their use as secondary flux calibrators. The sample was monitored as often as technical, weather and other time constraints allowed during night-time (Local time 16:00-08:00), complemented by day-time observations, if possible given technical constraints. During the more recent science operation phase, the first night in each block (both science and CSV) has been reserved to perform monitoring as part of the regression tests. Given night-time availability of a source, the aim was to obtain a minimum of one measurement at Band 3 every two weeks and one measurement at Bands 6 and/or 7 every two weeks. Observations at Band 7 were preferred. However, Band 6 measurements were obtained if weather constraints on submillimeter observations were in place (see the next section or memo 2 for a more detailed description of the monitoring strategy).

The monitoring program was initiated already in June 2010, but regular observations started in June 2011. Thirty-one of the 45 sources were successfully monitored at bi-weekly intervals, while the remaining were monitored at longer intervals up to 5 months. Most sources north of  $20^\circ$  were among those not monitored regularly. The number of antennas, the array configuration and weather conditions varied greatly over the course of the monitoring period. However, with as few as five antennas, accurate flux density measurements could be obtained.

Table 1: Spectral Window Frequencies for calibrator measurements in Bands 3, 6 and 7.

Receiver	Frequency				Database Frequency		Sensitivity <sup>1</sup> [mJy/min]
	LSB 1 [GHz]	LSB 2 [GHz]	USB 1 [GHz]	USB 2 [GHz]	LSB [GHz]	USB [GHz]	
3	97.5	99.0	109.0	110.5	98.25	109.25	2.0
6	221.5	220.32	234.5	236	228.075 <sup>2</sup>		3.3
7	336.5	338.0	348.5	350.0	343.25 <sup>2</sup>		5.2

<sup>1</sup> Under typical weather conditions for that band.

<sup>2</sup> Database frequencies are averaged for Bands 6 and 7.

### Wide Quasar sample

A large number of calibrators are needed in order to calibrate the shorter term gain and phase changes, which rely on a separation to the scientific target as little as possible. In order to find one of these calibrators within a few degrees of any place in the ALMA-visible sky, more than 1000 sources, evenly distributed, are required. Extensive lists of calibrator sources were available, mainly from low frequency surveys less than 43 GHz (VLA, at20g), with some high frequency data from the SMA and Planck (Planck Collaboration et al., 2011b).

The candidate list was constructed using the above databases to find those that might have a flux density greater than 1.0 Jy at 95 GHz. A first sample of about 600 candidate sources were selected based on their strength and position in the sky. Additional candidates were added within 10° of known targets that would be observed in the ALMA Cycle 0 and Cycle 1 projects. This entire sample of sources is denoted as the *wide* quasar sample. It is not meant to be complete in any respect, and it is continually being enlarged since it is important to use a quasar calibrator that is as close to the target as possible. The main criterion is that the calibrator be detectable at the 10-sigma level per antenna gain determination for a one-minute integration.

Between August 2011 and August 2013, the flux densities of these quasars were observed and the results placed into the ALMA catalog. Observations to enlarge the wide quasar sample have continued into the operational phase of ALMA and will be progressing for the next several years. In addition, monitoring these sources is being performed to update flux densities older than 1 year. At 95 GHz, using an array with 32 12-m antennas and a 2-GHz bandwidth, both polarizations, an acceptable flux density level is 0.1 Jy. There are an estimated 7,000 sources in the sky that meet this criterion. The goal is to provide sufficiently strong calibrators every 3-4 degrees for any point in the sky. ALMA observations over a large area of sky, and targeted searches near potential ALMA targets will be continuously performed during the operational phase.

# Observational Strategy and Data Reduction Methods

## Observing Frequencies

The flux density measurements for the grid sources were made at at least two frequencies in order to determine the spectral slope of each source so that its flux density could be estimated at all ALMA frequencies. The lowest frequency Band 3 (95 GHz) is an obvious choice where: (1) quasars with a negative spectral index are strongest; (2) The ALMA sensitivity is greatest; (3) the weather effects are smallest; (4) most instrumental effects are stable. The second frequency chosen was band 7 (350 GHz) which provides a large frequency lever arm from band 3. ALMA sensitivity is still good, and weather conditions are suitable at the ALMA site more than 40% of the time. When time permitted or if the weather was not optimum, Band 6 (230 GHz) observations were carried out. The observing set-ups and other observing parameters for the three frequencies are given in Table 1. Also included is the rms sensitivity for a 1 minute scan at each of the three bands under typical conditions with 12 antennas. All four 2-GHz basebands (two in each sideband) were used during all observations. Observations were done in full polarization (XX, YY, XY and YX) mode in preparation for the polarization capabilities of ALMA. This configuration gives 64 channels over each of the four 2 GHz bandwidth and two polarizations.

The number of available antennas and their locations were secondary for both types of observations, with five antennas the minimum number. Typically, 10 to 16 antennas were included. Because virtually all of the quasars are point sources, any configuration was satisfactory from the 20-m ACA baselines to the 1000-m ALMA baselines. Only when solar system objects were observed (see below), did the configuration play an important role. Some quasars do show structure. This will be discussed in more detail in the data reduction section.

## Observation Strategy

For the Grid sample, the sources were separated into six observing groups spread over about four hours in right ascension. Each group contained from 8 to 10 quasars. Consecutive groups had one quasar in common for redundancy. The six groups were made at Band 3, 6 and 7 and contained the same source selection. Each group/frequency observation is called a session which lasts from 45 min to 60 min. Each source was observed once.

Each session contained the following scans:

1. Focus and pointing offsets were determined at the beginning of each session were made at all bands. Only for bands 6 and 7, pointing offsets were determined for each source scan. At band 3 this was not necessary.
2. Integration times were longer at the higher frequencies because of the relative weakness of most quasars and the less sensitive system.
3. The system temperature was determined at the beginning of each scan. The calibration is important in removing the receiver and sky contributions to the system sensitivity and the amplitude levels.
4. No elevation correction was made for any dish efficiency change. Even at band 7, the estimated efficiency is  $< 3\%$  at  $30^\circ$  elevation.

In order to determine the *absolute* flux density of the grid quasars, a solar system object with a known flux density model was included as the first scan, **when possible**. The list of SSO's that have models good to 10% and are not too large in angular size are: Neptune, Uranus, Titan, Callisto, Ganymede, Mars and Pallas. Pointing, focus and system temperature measurements were made at the beginning of each SSO scan.

About one-third of the time, no SSO was available (in most cases, SSOs were too resolved to be used or too close to the planet in case of the Jovian moons or Titan) and grid observation would not be run. However, as more confidence was obtained in the flux density values measured in previous observations, the grid observations were run with no SSO, and a flux density for one of the quasars was assumed from the previous run(s). The uncertainties in the absolute flux density scale from this hybrid approach are discussed in this memo and in memo 2.

The wide quasar observations had similar observing structure and parameters to the grid observations. The majority of them were run only at band 3. The sessions began with an SSO object and a grid quasar that had a well-determined flux density. If a SSO object was not available, the grid calibrator provided the absolute amplitude scale. The remainder of the session consisted of 4 to 12 objects that were within about 30° of the grid calibrator. The sources observed were either data filling of potential calibrators over this part of the sky, or the checking of particular calibrator candidates that were close to targets that were going to be observed by ALMA.

## Data Reduction/Pipeline

Each session was calibrated, edited, imaged and analyzed independently, using an up-to-date version of CASA (Jaeger, 2008). The results were generally available (inserted into the ALMA catalog) from one day to one week after the session. This fast turn around was important in order for the reduction of the early science data to have the flux density of the grid source if it was needed as the flux calibrator for the observation.

The initial reduction script developed into a semi-automatic pipeline with python scripts connecting the CASA tasks. Many displays and tables were generated in order to assess the problems and quality of the data. A description of this pipeline is on the Twiki of the ALMA Department of Science Operations: <https://wikis.alma.csi.cornell.edu/view/DSO/HowToReduceCalSurveyData>. The main steps in the reductions are as follows:

1. Convert the archive data into a measurement set.
2. Apply a priori calibrations and flagging.
3. Choose one quasar as the main calibrator and determine bandpass and amplitude scale, assuming the quasar is 1.0 Jy
4. Average the 64 frequency channels in each spw
5. phase self-calibrate each scan to remove tropospheric phase fluctuations
6. Average the scan for each baseline
7. If a SSO was observed, the ratio of its calibrated visibility (based on the 1-Jy calibrator) to its model visibility gives the scaling factor needed for each spw/pol. Only SSO visibility data before the model visibility dropped below 20% due to resolution effects were used. For very resolved SSO, perhaps only 3 to 5 baselines were available.
8. If no SSO object was observed, then the flux density scale is determined by the flux density assumed for the main calibrator from a different origin.
9. The flux densities of all of the sources were then determined from the average of the corrected baseline visibility amplitudes.
10. The measurement error was obtained as follows :First, the rms flux error per baseline was determined. This error was then divided by the square-root of the number of antennas used for the source. Regardless of the above results, a lower limit flux density error of 3% at band 3 and 5% at bands 6 and 7 of the total flux was applied. A detailed discussion about the error estimates is given below.
11. An estimate of the percentage polarization was determined for each source by the combination of the four visibility amplitude correlations:  $\sqrt{((XX-YY)^2 + (XY+YX)^2)}$ . The only polarization calibration was to remove the delay between the XX and YY correlations so that the XY and YX values were coherent over each spw.
12. For Band 3, a flux and error estimate was obtained for the lower sideband and upper sideband separately since the frequency difference is 10%. All four spw were average for band 6 and band 7. Both linear polarizations were combined.

The typical output from the pipeline is shown below. It can be ingested directly into the ALMA catalog using XMLRPC scripts. It has the following entries: Source name, RA, RA error, Dec, Dec error, Center frequency, flux density, statistical flux density error (see below on assessment of flux density errors), percentage of polarization, error on polarization percentage, angles, structure in the form of UVMIN and UVMAX, and date of observation. 'NE' means No Entry. For some sources, more commonly accepted names are used mainly for historical reasons. The J2000 names and accurate positions are correctly associated with the common names in the database. UVMIN = 0.0 means that no large-scale emission has been detected yet. UVMAX = -XX means that at a baseline length of XX wavelengths, no resolution. Notice the 3c273 has large-scale structure which is seen in the visibility data when less than 20 k $\lambda$  is observed. Positions are currently labelled as NE. It is possible to derive positions of quasars in the future, if required.

```
*****
SOURCE      RA RAE DEC DECE   FREQ    FLUX FLUX_E %POL %PERR PANG UVMIN UVMAX  DATE OBS
J1037-295,  NE, NE, NE, NE,  343.48E+09,  0.56, 0.04, 0.06, 0.03, NE, NE,  0.0, -1470.1, 2013-12-11
J1058+015,  NE, NE, NE, NE,  343.48E+09,  1.42, 0.10, 0.07, 0.04, NE, NE,  0.0, -1367.3, 2013-12-11
J1107-448,  NE, NE, NE, NE,  343.48E+09,  0.63, 0.05, 0.04, 0.03, NE, NE,  0.0, -1466.8, 2013-12-11
J1146+399,  NE, NE, NE, NE,  343.48E+09,  0.80, 0.07, 0.06, 0.05, NE, NE,  0.0, -1320.7, 2013-12-11
  3c273,    NE, NE, NE, NE,  343.48E+09,  1.91, 0.14, 0.02, 0.02, NE, NE, 20.0, -1196.6, 2013-12-11
  3c279,    NE, NE, NE, NE,  343.48E+09,  7.77, 0.35, 0.09, 0.03, NE, NE,  0.0, -1160.7, 2013-12-11
J0854+201,  NE, NE, NE, NE,  343.48E+09,  1.51, 0.08, 0.05, 0.03, NE, NE,  0.0, -1470.4, 2013-12-11
J0635-751,  NE, NE, NE, NE,  343.48E+09,  0.36, 0.05, 0.08, 0.08, NE, NE,  0.0, -1327.4, 2013-12-11
*****
```

Because most Grid and Wide calibration sessions have 15 or more antennas and point sources are being observed, very strict standards in consistency can be applied in order to remove data that is marginally suspect. After the first pass through the pipeline, there are many plots and tables from which outliers can be detected. The strongest comparison is the derived flux density for each source for each antenna/spw/pol. For a point source, the flux density should be the same and any errant antenna can be easily spotted and removed. Examples: If the pointing is not optimum for an antenna, then the relative gains of the antenna for each source will vary more than the other antennas; If the tsys of an antenna is anomalous high or much more variable with elevation than other antennas. Because of the redundancy of the data in obtaining flux densities of point sources, flagging such marginal data will produce more accurate results.

## Source structure

Most sessions have sufficient u-v coverage, even with one scan, to determine any large or small scale structure associated with the quasar. Because even a small amount of contaminating data or large phase fluctuations can suggest false source structure, several methods are used to determine non-point like emission of the quasar. These are judged by the reducer and resolution effects are manually inserted into the ALMA data base. At the present time only about 10 sources out of about 500 well-studied sources are sufficiently non-point like. Even these affect the calibrations at the 3% and 5° level.

The three methods to determine if there is source structure are:

1. The pipeline determines the flux density and estimated error of each source in three u-v ranges: flux-short, flux-med and flux-long. If flux-long is less than 85% of the average of the other two, a warning statement is given in the form above that the source may be resolved at long baselines
2. If the flux-short rms error is significantly larger than the other two errors, then a warning statement is given in the form above that the source may have large-scale structure. Since large-scale structure tends to produce fluctuating correlated flux densities at the short baselines (rather than a simple increase in correlated flux density), this criterion is used.
3. Images are routinely made of all observed sources. Large-scale structure is often obvious in the image display.
4. For a source that is suspected to be resolved at long baselines, the plot of correlated flux density versus uv-distance should confirm the resolution suggested by the pipeline. Often, the loss of long baseline flux is a coherence problem when the phase fluctuations are large.

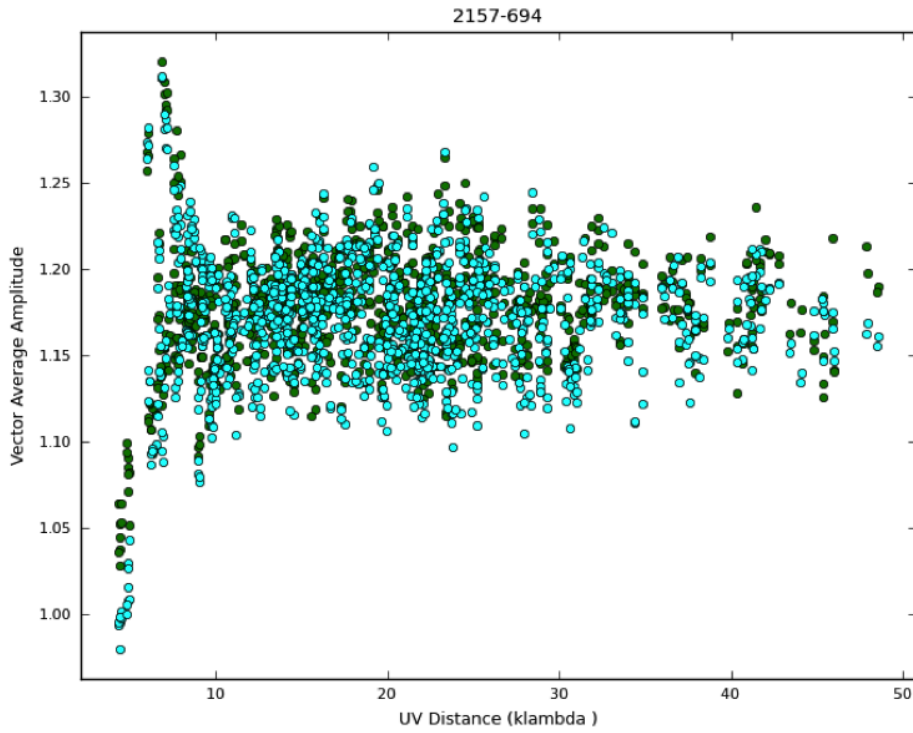
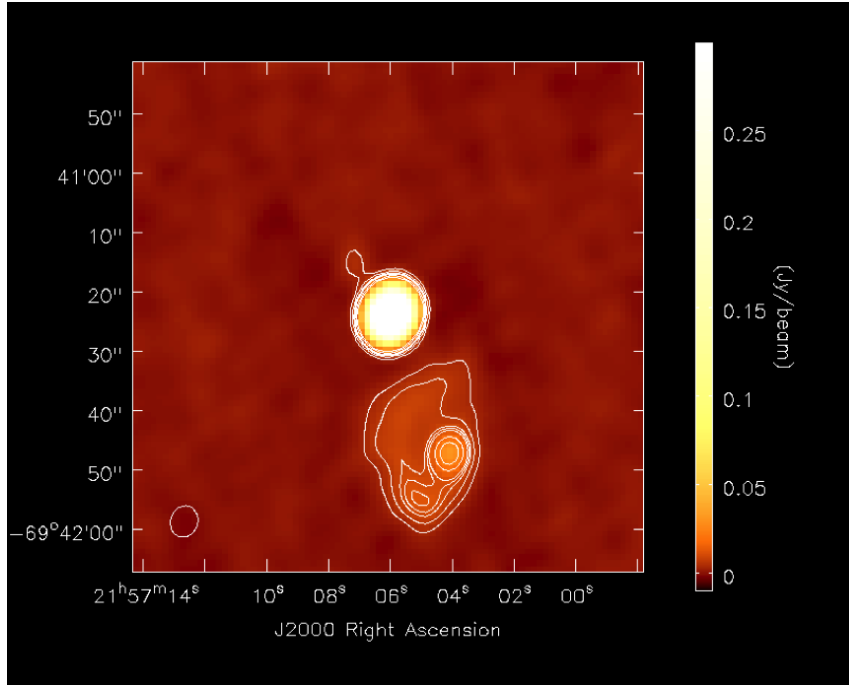


Figure 4: Example of source structure in J2157-694. The emission is dominated by the central unresolved component, but the large-scale emission from the jet is significant (30% or higher), decorrelating emission for baselines under 10  $k\lambda$ .

An example is shown in Fig. 4. However, using these calibrators with no correction for structure, still is able to produce amplitude gain calibrations in error by a few percent and phase gain calibrations in error

by less than five degrees.

Source structure is a minimal problem with the current ALMA configurations. When longer baselines (>3 km) become available, where non-point like thermal sources may be of use at higher frequencies, structure will become more of a problem. Identifying structures at this stage will aid future efforts.

### **Assessment of Flux Density Errors**

The flux density errors given in the output table from the reduction pipeline are derived from the internal error per point, divided by the number of independent points. This number is the square-root of the number of antennas or the fourth-root of the number of baselines. A minimum error, however, of 3% at band 3 and 5% at bands 6 and 7 is used to include systematic error contributions that are difficult to quantify. More conservative estimates produce errors up to 6% in Band 3, and up to 10% in Bands 6 and 7.

We compared the spread of the measured flux densities of the sources over time with the errors that are quoted from each session. The results suggest that the error estimates are reasonable. The analysis will be presented in a future memo. The various potential origins are listed below, in order of importance and scale of uncertainty. Some of these uncertainties have been reduced during regular operations from the conclusions drawn from the monitoring programs.

#### **Uncertainty from planetary models**

The most serious errors arise from the uncertainty in the planetary model or the uncertainty in the assumed main quasar flux density if that is used. At the beginning of the flux density monitoring, it was clear that the solar system models were compatible only at the 10% level, and that some SSO's had significant narrow (Titan) or wide absorption features (Neptune) in one or more of the spw's. Neptune was selected as the main reference for amplitude calibration. Improvements in the SSO models were made two years ago (called 'Butler JPL-Horizon 2012' in CASA). This means that the derived flux density of a quasar can vary by up to the current error of the model, depending on the SSO that is used. If a quasar flux density is used for the amplitude scaling, this uncertainty is somewhat larger than 5% even in cases when the quasar has had measurements within the last month. ALMA observations are now underway to reduce the model differences among the solar system objects and to include asteroids and well-modeled stellar sources. For older observations, models in CASA 3.2 or earlier were used. As such, errors introduced by planetary models are on average twice as high.

#### **System temperature measurements**

A system temperature is measured at the beginning of each scan. Any errors in the applied system temperatures—that are scale factors for each scan—will be translated into a flux density error. Errors are more susceptible for observations lower than about 40° elevation.

#### **Radiometer corrections on the short-term phase solutions**

Radiometers near 180 GHz on each antenna measure the water vapor emission along the line of sight to the source. The emission can be converted into path delay and this system is very effective at removing short-term phase fluctuations from one second to a few minutes of time. Any remaining phase fluctuations are removed by the self-calibration phase processing. Only in poor conditions is there significant coherence loss at longer baseline lengths (seeing limit) which give an apparent size to the source.

#### **Pointing Errors**

Erroneous pointing can significantly increase statistical errors on derived flux densities. The pointing tolerance of ALMA is 2 arcseconds at any position in the sky above 20 degrees elevation. At Band 3, this corresponds to 98.5% of optimum sensitivity. Even at Band 7, the sensitivity of the antennas should still be ~95%. However, if the pointing offset is a constant collimation error over the sky, than the loss of sensitivity will be similar for all sources and cancel out in the calibration. If the pointing error produces different gain changes between sources, it will be seen in the pipeline output (see above) and the antenna data can be flagged. Although performing pointing scans on the sources themselves could easily calibrate these errors, the amount of integration time needed to perform a pointing during commissioning was considered

to be too costly. Pointings effectively took 2 minutes, compared to the actual integration time of 30 to 90 seconds.

### **Focus Errors**

The focus parameters for each ALMA telescope are measured weekly and should not produce amplitude errors among the sources by more than a few percent. As with residual pointing errors, only differential focus offsets among sources at different times and elevation will affect the results since a constant loss of efficiency will be calibrated out. The Y focus updates automatically with the elevation based on pre-determined focus curves.

## Results

### Monitoring of the Grid Sample

Table 2 gives the list of grid sources that were being actively monitored during the fall of 2013, with measurements up to date to mid-2013. At this time, the monitoring program was part of regular operations. This list has changed and will keep on changing with time: sources getting weaker over significant periods of time will be dropped and replaced by other bright quasars in the same region of sky. For the most up to date flux density values of these sources, please consult the web interface.

The distribution of the Grid sources is shown in Figure 5. The median separation between sources is 25 degrees. With this distribution, at least one grid source is above 30 deg elevation at any time of the day; hence one should be available for bandpass calibration and/or flux density scaling for any target.

### Flux density history

The cadence of the grid observations allows for detailed flux density histories to be constructed and thus quantify variations over time. The flux density history of J1924-292 from April 2011 up to May 2014 is shown in Fig. 6. A range of variabilities is seen of various amplitudes and covering various timescales: small variations are seen on timescales of days to a few weeks, while a large variation extends to the full three years during which observations were obtained. J1924-292 has dimmed by more than a factor 2 in the last two years, but is recently brightening again. Note that the dimming is independently seen in Bands 3, 6 and 7.

### Wide sample

Currently, flux densities of nearly 700 quasars have been measured by ALMA. Virtually all have been measured in Band 3, at both 95 and 109 GHz. About half also have measurements at higher frequencies (most often Band 7). The sky coverage for Band 3 is shown in Figure 7. Some areas have not been covered extensively, often because of the concentrated search for calibrators near certain science targets, LST access or conflicts with other commissioning efforts. The median separation of a random point on the sky to a calibrator is  $3.5^\circ$ . In addition, there is a 90% probability of finding a calibrator within  $7^\circ$  (see Fig. 8, reproduced from Fomalont et al., 2014, ESO Messenger 155). This will decrease substantially as more quasar calibrators are confirmed in the coming years.

### Spectral Index

If measurements are taken in multiple bands within a relatively short period of time, the spectral index of a quasar in the ALMA frequency range can be derived. Generally, measurements taken at different frequencies within fourteen days can be compared to obtain a reasonably accurate spectral index. Larger time separations introduce uncertainties in the slope which are affected by potential intrinsic time variations. A detailed analysis of the frequency and temporal separation of the quasar flux densities will be presented at a later time.

During the 2011 to mid-2013 period, 151 measurement pairs with separation less than 14 days were obtained for Band 3 and 6, 119 for Band 3 and 7 and 64 for Band 6 to 7. The flux densities of the measurement pairs of Band 3 and 6 are shown in Fig. 9. The slope of this correlations provides a mean spectral slope for quasars at ALMA wavelengths. The average  $\alpha$  values are -0.70 for Band 3 to 6 and -0.59 for Band 3 to 7 and -0.70 for Band 6 to 7. Note that multiple measurement pairs associated with the same source are included.

The spectral indices agree well with that expected from synchrotron emission, with little indication of thermal emission contribution. Very few sources have a flat spectrum with  $\alpha \approx 0$ : only four sources between Bands 3 to 6 and just one between Band 3 to 7. At cm-wavelengths, flat spectrum radio emission is caused by emission from optically thick radio emitting regions; flat spectrum radio emission at tera-Hertz frequencies is caused by thermal emission. From these spectral slopes, it can be concluded that at the ALMA frequency range, nearly all quasar emission is from optically thin synchrotron emission.

We are aware that the rough derivations above have their limitations. Several observations of 18-26 hours duration have been made on the calibrator sources at bands 3, 6 and 7. From these data a spectral index and spectral curvature can be determined reliably since there is virtually no time difference between the

Table 2: Flux density measurement in Bands 3,6 and 7 of the ‘bright’ or ‘grid’ sample of 45 quasars. The table list the flux densities, their errors and the date of the observation of Bands 3, 6 and 7.

Source	Band 3			Band 6			Band 7		
	Flux Density	Error	Date	Flux Density	Error	Date	Flux Density	Error	Date
J0106-405	0.620	0.030	20120112	0.300	0.010	20110726	0.220	0.030	20111013
J0132-169	1.290	0.070	20120807	0.890	0.040	20110726	0.780	0.050	20111013
J0237+288	1.830	0.060	20130701	1.590	0.110	20121020	0.770	0.100	20130702
J0238+166	0.910	0.050	20130708	0.960	0.050	20121006	0.480	0.060	20130702
3C84	15.500	1.200	20130708	10.210	0.690	20121020	6.570	0.390	20130705
J0334-401	0.970	0.060	20130708	0.980	0.050	20121006	0.400	0.040	20130702
J0423-013	3.420	0.170	20130701	3.600	0.220	20121020	1.590	0.110	20130705
J0510+180	3.630	0.130	20121216	2.090	0.090	20121019	2.180	0.120	20121202
J0519-454	1.750	0.040	20121216	1.180	0.060	20121019	1.010	0.050	20121202
J0927+390	4.740	0.240	20111111	-	-	-	1.730	0.090	20111113
J1037-295	0.690	0.020	20130705	0.830	0.040	20121006	0.540	0.040	20130417
J1058+015	1.630	0.070	20130705	1.580	0.080	20121006	0.800	0.070	20130417
J1107-448	1.470	0.050	20130705	0.750	0.040	20121006	0.650	0.060	20130417
J1130-148	1.300	0.070	20111111	-	-	-	0.490	0.060	20120615
J1146+399	0.990	0.070	20130705	-	-	-	0.390	0.050	20130417
J1147-6753	1.070	0.070	20120125	0.580	0.040	20111118	0.700	0.050	20111115
J1159+292	0.700	0.040	20120307	-	-	-	0.450	0.040	20111204
3C273	6.990	0.540	20130705	2.950	0.150	20121006	2.220	0.110	20130510
3C279	17.690	1.030	20130705	13.070	0.650	20121006	6.300	0.280	20130510
J1337-129	5.930	0.200	20130705	4.140	0.210	20121006	2.540	0.070	20130510
J1426+364	0.330	0.020	20120307	0.170	0.010	20110613	0.150	0.030	20111204
J1427-421	7.450	0.180	20130705	3.930	0.200	20121006	4.100	0.320	20130510
J1517-243	1.680	0.050	20130705	1.290	0.060	20121006	0.820	0.090	20130510
J1550+054	1.050	0.080	20130705	0.590	0.030	20121006	0.380	0.040	20130703
J1613-586	1.400	0.040	20130702	1.170	0.060	20121006	0.540	0.040	20130703
3C345	3.000	0.120	20130702	1.680	0.080	20110613	1.160	0.100	20130702
J1733-130	2.390	0.060	20130702	1.660	0.080	20121006	0.910	0.060	20130703
J1751+096	2.700	0.090	20130702	2.250	0.110	20121006	1.280	0.090	20130703
J1924-292	5.350	0.170	20130702	3.970	0.130	20121022	2.520	0.130	20130703
J2025+337	2.060	0.060	20130702	1.050	0.050	20110724	0.890	0.070	20130703
J2056-472	1.010	0.040	20130702	0.990	0.040	20121022	0.470	0.050	20130701
J2148+069	2.280	0.050	20130702	1.010	0.050	20121006	0.630	0.040	20130703
J2157-694	1.300	0.080	20120124	0.880	0.040	20110724	-	-	-
J2202+422	8.910	0.450	20111031	2.720	0.140	20110724	-	-	-
J2232+117	3.290	0.190	20130702	4.890	0.250	20121022	1.380	0.090	20130701
3C454.3	3.530	0.180	20120324	2.470	0.130	20111126	1.720	0.090	20111116
J2258-279	1.650	0.100	20130702	3.250	0.130	20121020	0.590	0.040	20130702
J2357-5311	1.070	0.050	20130708	0.780	0.060	20121020	0.430	0.040	20130702

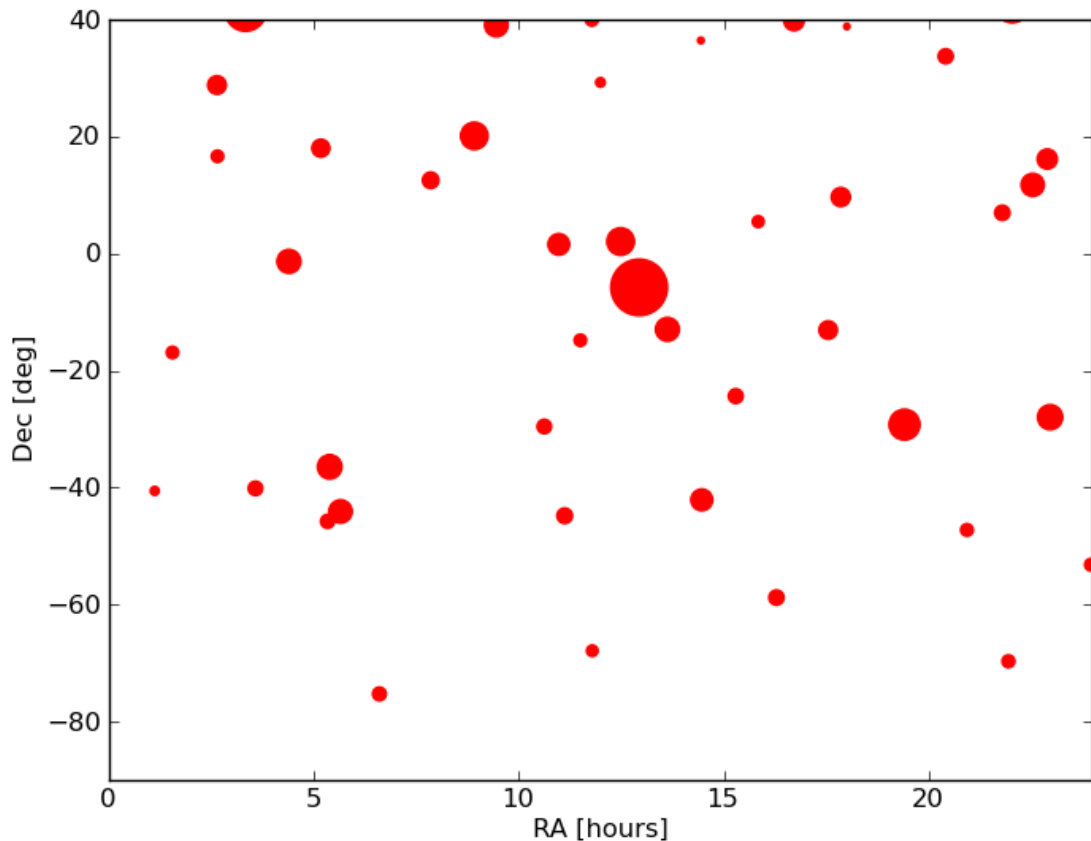


Figure 5: Sky locations of the bright quasars in the monitoring sample. Points are scaled by the most recent Band 3 flux density. The smallest circles correspond to sources with a flux density 0.5 Jy or less.

observations. Such observation runs will become more frequent in the future because it is more efficient to observe all calibrators in one long session than to break the flux monitoring observations into many pieces that are fit into the overall observing schedule when possible. Also, the determination of a source spectral curvature will provide better frequency interpolation to other frequencies, especially band 9. Analyses of these runs will be presented at a later time, including derivations of spectral indices.

### Frequency Inter- and Extrapolation

Since the derivation of the continuum spectral slope of quasars is relatively simple, but with only a relatively small scatter, flux densities at frequencies that have not been directly measured can be estimated from two radio observations at lower frequencies. This is especially useful for estimating flux densities at Band 9 (~690 GHz) without the need to spend valuable good weather conditions on flux density measurements. For ALMA, pairs of band 3 (95 GHz) and band 7 (350 GHz) observations are best suited, leading to about a 5% accuracy in the estimate.

At the highest ALMA frequencies, above 600 GHz, the flux density of only a handful of quasars is sufficiently high to be reliable bandpass calibrators, and use of a phase calibrator that is only marginally strong will decrease the value of an observation due to errors in the gain calibration. Although it is possible to monitor the flux density of calibrators at band 9 (650 GHz), observing time at these higher frequencies are at a premium and scientific projects have first priority.

The estimated Band 9 flux densities can be extrapolated from a Band 7 flux density and the spectral index. In July 2011, this extrapolation technique was tested by observing 8 quasars of the bright sample for 2 minutes using Band 9 and comparing the derived flux densities to those predicted from extrapolation of flux densities obtained with Band 6 in the same week. We observed at 660 and 674 GHz where the

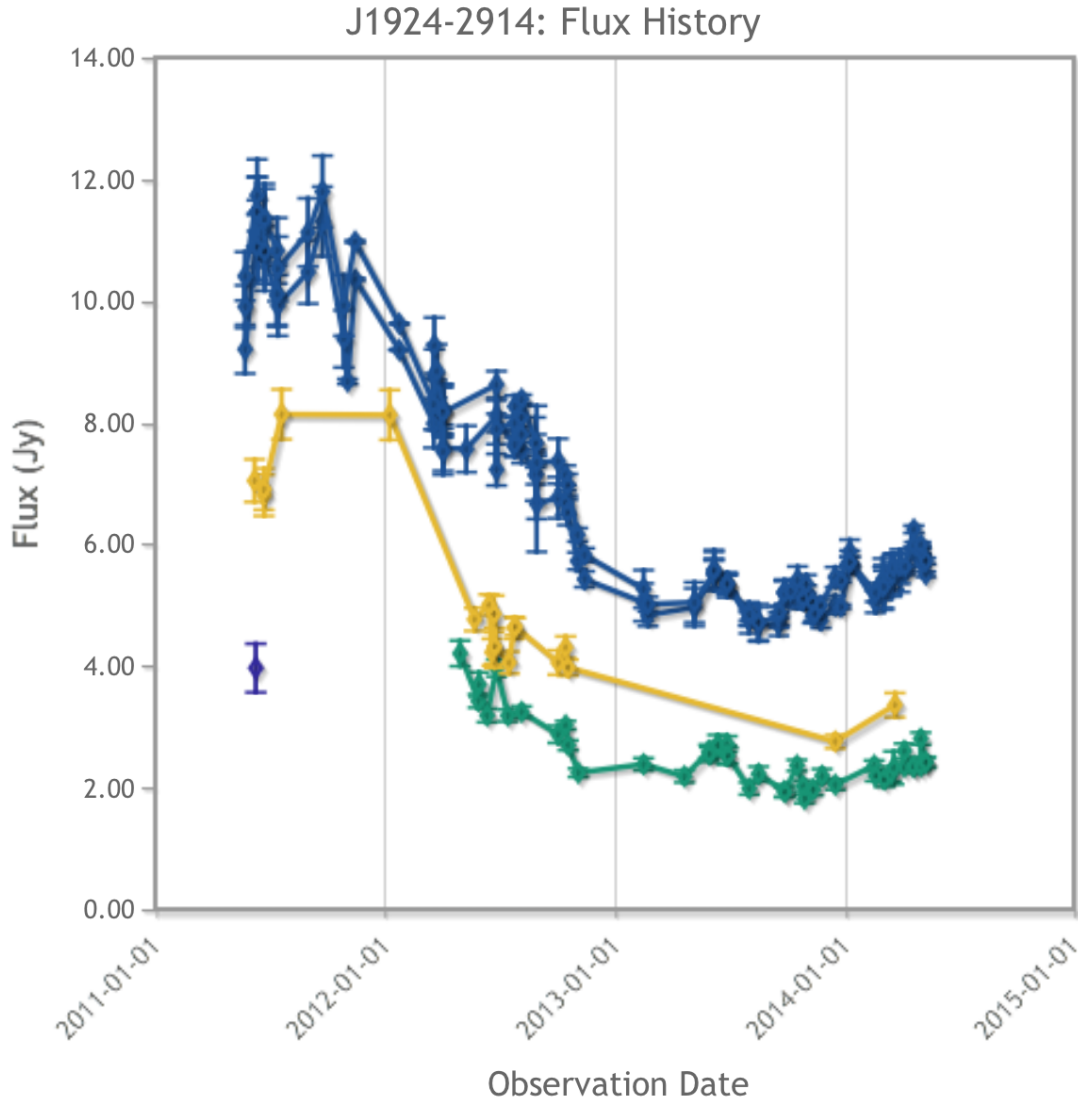


Figure 6: Example of a flux density history of a regularly observed ‘grid’ source (J1924-292, also known as J1924-2914). Figure is taken from the web-based interface. Blue points are the Band 3 flux densities, yellow the Band 6 flux densities, green the Band 7 flux density and the lone purple point (mid-2011) is a measurement taken using Band 9.

atmospheric window is clearest and where there are no strong emission lines. Neptune was used as the absolute flux calibrator in both the Band 6 and Band 9 observations to reduce any systematic errors. The extrapolated flux density predictions were derived by using

$$F_{667} = F_{228} \times (667/228)^\alpha \quad (1)$$

with values of both -0.59 and -0.7 for  $\alpha$ . All flux densities, as well as differences between the measured and extrapolated flux densities in Band 9 are listed in Table 3.

Most predicted flux densities differ by 5 to 15 % from the measured flux density. With similar uncertainties in absolute flux calibration using Neptune, as well as Band 9 system gain uncertainties, the result shows that the extrapolation to Band 9 is sufficiently accurate *to assess the viability of a source as a detectable phase calibrator*.

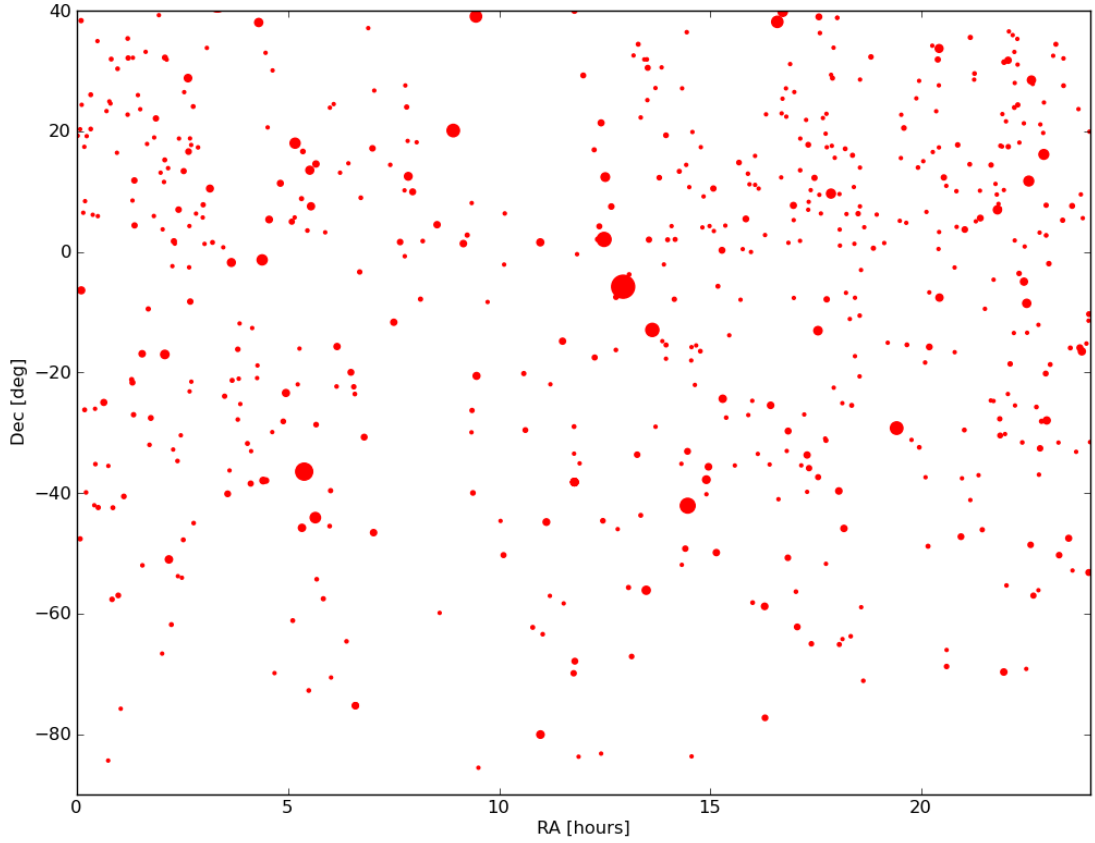


Figure 7: Positions of all quasars observed in the ‘wide’ sample observed with ALMA in Band 3. Points are scaled to the most recent flux density measurement, and normalized to the brightest source (3C279).

Table 3: Measurements of Band 6 and 9 flux densities compared to predicted values through extrapolation from Band 6 using  $\alpha = -0.6$  and  $-0.7$

Source	Observed flux density		Predicted flux density			
	Band 6 [Jy]	Band 9 [Jy]	$\alpha = -0.6$ [Jy]	Dev. <sup>1</sup> [%]	$\alpha = -0.7$ [Jy]	Dev. <sup>1</sup> [%]
J1924-292	6.80	4.00	3.47	-15%	3.21	-25 %
J2025+337	1.07	0.47	0.55	+14%	0.51	+8%
J2056-472	0.92	0.50	0.47	-6%	0.43	-16%
J2148+069	0.77	0.32	0.39	+18%	0.36	+11%
J2157-694	0.80	0.46	0.41	-12%	0.38	-21%
J2203+317	0.76	0.34	0.39	+13%	0.35	+3%
J2232+117	0.60	0.31	0.31	0%	0.28	-10%
3C454.3	6.46	3.34	3.29	-2%	3.04	-10%
J2258-279	1.73	0.95	0.88	-8%	0.81	-17%
Average deviation				0.2%	-9%	
Average absolute deviation				9.8%		13%

<sup>1</sup> Deviation from the measured Band 9 flux density. A minus sign indicates the predicted flux was an underestimate.

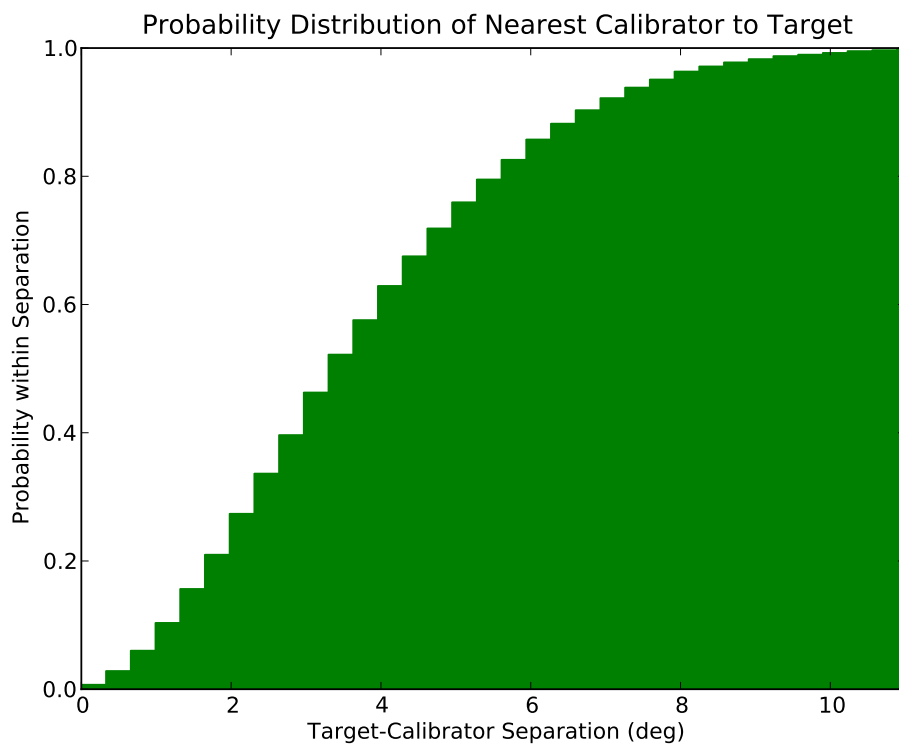


Figure 8: Histogram of the Target-Calibrator Separation from the ALMA calibrator database. The probability distribution for the minimum separation of a random position in the sky from the nearest Band 3 calibrator is shown. The distribution was binned to 0.33 degrees. The median separation is  $3.5^\circ$  and there is a 90% probability of finding a calibrator within  $7^\circ$  of a random target.

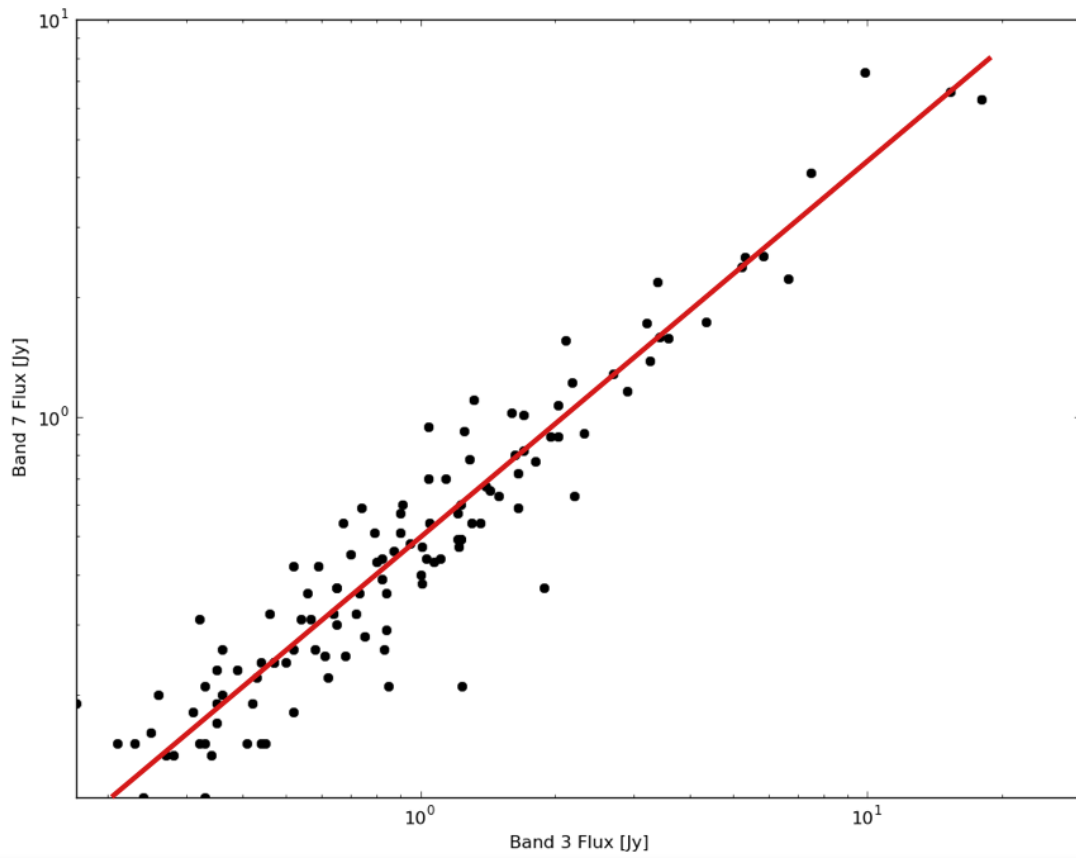


Figure 9: Flux Densities obtained at Band 3 and Band 7 within 14 days or less. The red line is the best fit, resulting in a slope of 0.59.

## Summary

In this memo we presented the ALMA calibrator database and the work done in filling it with quasar flux densities. The motivation and results of the monitoring program of a sample of 45 quasars (the *grid* sample) and the determination of the flux densities of  $\sim 650$  quasars (the *wide* sample) were described. Variability with time and extrapolation of the flux densities, especially to frequencies above 600 GHz, were subsequently discussed. The main conclusions in the memo can be summed up as follows:

- Over 600 quasars were observed in order to build an initial calibrator database for ALMA, necessary to provide information on potential gain calibrators. During the operational phase of ALMA, new measurements will be added.
- A group of 45 bright quasars, distributed evenly over the sky, was monitored as regularly as possible over a period of two years to provide strong sources for accurate calibrations, especially at narrow bandwidths. This monitoring program has continued into the operational phase.
- We show that the grid sources are candidates for flux density calibration, providing a solution to long baseline flux calibration.
- The pipeline script was described.
- Origins for uncertainties in calibrator flux density measurements were discussed.
- Using observations of quasars in multiple bands, average spectral slopes between 3 mm and 0.85 mm were derived for a large number of quasars.
- The mean spectral slopes were used to extrapolate Band 6 flux densities to Band 9. These were compared with observed flux densities at 668 GHz taken in the same week. Accuracy of this extrapolation was  $\sim 15\%$ . This technique can be applied to select or weed out potential calibrators for high frequency observations.

## Acknowledgments

This effort could not be completed without the hard work of many people involved in the commissioning of ALMA, especially those of the commissioning and science verification (CSV), the science operations (DSO), as well as the array operations (AOG) groups. The authors would like to thank the entire scientific JAO staff for making this work possible.

## References

- A J Beasley, D Gordon, A B Peck, L Petrov, D S MacMillan, E B Fomalont, and C Ma. The VLBA Calibrator Survey-VCS1. *The Astrophysical Journal Supplement Series*, 141(1):13–21, July 2002.
- D O Edge, J R Shakeshaft, W B McAdam, J E Baldwin, and S Archer. A survey of radio sources at a frequency of 159 Mc/s. *Mem. R. Astron. Soc.*, 68:37–60, 1959.
- E B Fomalont, L Petrov, D S MacMillan, D Gordon, and C Ma. The Second VLBA Calibrator Survey: VCS2. *The Astronomical Journal*, 126(5):2562–2566, November 2003.
- M A Gurwell, A B Peck, S R Hostler, M R Darrah, and C A Katz. Monitoring Phase Calibrators at Submillimeter Wavelengths. *From Z-Machines to ALMA: (Sub)Millimeter Spectroscopy of Galaxies ASP Conference Series*, 375:234, October 2007.
- S Jaeger. The Common Astronomy Software Application (CASA). *Astronomical Data Analysis Software and Systems ASP Conference Series*, 394:623, August 2008.
- Marcella Massardi, Ronald D Ekers, Tara Murphy, Elizabeth Mahony, Paul J Hancock, Rajan Chhetri, Gianfranco de Zotti, Elaine M Sadler, Sarah Burke-Spolaor, Mark Calabretta, Philip G Edwards, Jennifer A Ekers, Carole A Jackson, Michael J Kesteven, Katherine Newton-McGee, Chris Phillips, Roberto Ricci, Paul Roberts, Robert J Sault, Lister Staveley-Smith, Ravi Subrahmanyan, Mark A Walker, and Warwick E Wilson. The Australia Telescope 20 GHz (AT20G) Survey: analysis of the extragalactic source sample. *Monthly Notices of the Royal Astronomical Society*, 412(1):318–330, March 2011.
- Bojan Nikolic, Sarah F Graves, Rosie C Bolton, and John S Richer. Design and Implementation of the wvrgcal Program. *arXiv.org*, July 2012.
- Alok R Patnaik, Ian W A Browne, Peter N Wilkinson, and Joan M Wrobel. Interferometer phase calibration sources. I - The region 35-75 deg. *Monthly Notices of the Royal Astronomical Society (ISSN 0035-8711)*, 254:655–676, February 1992.
- Planck Collaboration, J Aatrokoski, P A R Ade, and Planck Collaboration. Planck early results. XV. Spectral energy distributions and radio continuum spectra of northern extragalactic radio sources. *Astronomy and Astrophysics*, 536:15, December 2011a.
- Planck Collaboration, P A R Ade, N Aghanim, and Planck Collaboration. Planck early results. VII. The Early Release Compact Source Catalogue. *Astronomy and Astrophysics*, 536:7, December 2011b.
- Planck Collaboration, P A R Ade, N Aghanim, F Argüeso, and Planck Collaboration. Planck intermediate results. VII. Statistical properties of infrared and radio extragalactic sources from the Planck Early Release Compact Source Catalogue at frequencies between 100 and 857 GHz. *Astronomy and Astrophysics*, 550:133, February 2013.
- Joseph L Richards, Walter Max-Moerbeck, Vasiliki Pavlidou, Oliver G King, Timothy J Pearson, Anthony C S Readhead, Rodrigo Reeves, Martin C Shepherd, Matthew A Stevenson, Lawrence C Weintraub, Lars Fuhrmann, Emmanouil Angelakis, J Anton Zensus, Stephen E Healey, Roger W Romani, Michael S Shaw, Keith Grainge, Mark Birkinshaw, Katy Lancaster, Diana M Worrall, Gregory B Taylor, Garret Cotter, and Ricardo Bustos. Blazars in the Fermi Era: The OVRO 40 m Telescope Monitoring Program. *The Astrophysical Journal Supplement*, 194(2):29, June 2011.

## A Appendix: Flux Densities observed by ALMA during Commissioning

In this appendix, we list flux densities of over 600 quasars, measured in the period of 2010-2013. The list has been updated to include measurements up to October 2013. Since then many more quasars have been observed. Sources also have been reobserved during the operational phase of ALMA. The measurements of these sources were done during commissioning of ALMA, taking place before and during Cycle 0.

Table A.1: Flux densities of all calibrators in the ALMA calibrator database. Last updated on 2013-10-29.

Name	Band 3		Band 6		Band 7	
	Flux Density [Jy]	Date	Flux Density [Jy]	Date	Flux Density [Jy]	Date
J000109+191428	0.11	20120902	-	-	-	-
J000436-473610	0.51	20120408	0.28	20120623	-	-
J000435+201933	0.15	20120902	-	-	-	-
J0005+383	0.52	20120527	-	-	-	-
J0006-0624	1.56	20120530	-	-	1.1	20130723
J000649+242232	0.1	20120902	-	-	-	-
J000903+062820	0.18	20120527	-	-	-	-
J0010+174	0.25	20120527	0.12	20120902	-	-
J0011-2613	0.43	20120807	-	-	-	-
J001134+082360	0.1	20120527	-	-	-	-
J0012-399	0.35	20120530	0.22	20120623	-	-
J001356+191036	0.16	20120902	-	-	-	-
J0020+2022	0.39	20120527	-	-	-	-
J0019+260	0.43	20120902	-	-	-	-
J0023+0608	0.27	20120527	-	-	-	-
J002443-420202	0.02	20120902	-	-	-	-
J0026-2602	0.17	20120807	0.04	20120623	-	-
J0026-3512	0.35	20120530	0.13	20120623	-	-
J0029+3457	0.26	20120527	-	-	-	-
J0030+0555	0.2	20120527	0.1	20120902	-	-
J0030-4224	0.52	20120807	0.19	20120623	-	-
J0038-2459	1.14	20120530	0.56	20120623	-	-
J0042+2320	0.27	20120527	-	-	-	-
J0044-8423	0.17	20120807	-	-	-	-
J0045-3531	0.02	20120902	-	-	-	-
J004607+245627	0.23	20120527	-	-	-	-
J004743+243503	0.18	20120626	-	-	-	-
J004847+315718	0.42	20120626	-	-	-	-
J0050-5738	0.58	20120530	-	-	-	-
J0051-4227	0.44	20120807	0.24	20120623	-	-
J0056+164	0.14	20120527	-	-	-	-
J005748+302114	0.38	20120527	-	-	-	-
J0058-5659	0.65	20120609	-	-	-	-
J0102-7547	0.29	20120408	-	-	-	-
J0107-4034	0.62	20120112	0.3	20110726	0.2	20130723
J0112+2245	0.34	20120626	-	-	-	-
J0112+3522	0.39	20120626	-	-	-	-
J011250+320832	0.54	20120626	-	-	-	-
J0117-2111	0.47	20120807	0.23	20120623	-	-
J0119-2142	0.74	20120807	0.6	20120623	-	-
J0119+0830	0.14	20120626	-	-	-	-
J011935+321048	0.16	20120626	-	-	-	-
J0120-270	0.54	20120807	0.37	20120720	-	-
J0122+1150	0.86	20120626	-	-	-	-
J0122+0422	0.81	20120626	-	-	-	-
J0127+2559	0.25	20120625	-	-	-	-
J0129+236	0.1	20120625	-	-	-	-
J0133-1655	1.29	20120807	0.89	20110726	0.4	20130723
J0133-5200	0.35	20120807	0.19	20120902	-	-
J0138+3310	0.28	20120625	-	-	-	-
J013942+175253	0.11	20120625	-	-	-	-
J0141-0929	0.51	20120804	0.36	20120720	-	-
J0143-3201	0.35	20120609	0.25	20120720	0.19	20111013
J014504-273322	0.7	20120609	0.36	20120720	-	-

*Continued on next page*

Table A.1 – Continued from previous page

J0149+0556	0.32	20120625	-	-	-	-
J014949+185705	0.18	20120625	-	-	-	-
J0152+2207	0.83	20120625	-	-	-	-
J015632+391439	0.16	20120625	-	-	-	-
J015855+130705	0.17	20120625	-	-	-	-
J0201-6638	0.12	20120807	0.06	20120902	-	-
J020151+034307	0.05	20120626	-	-	-	-
J0204+1135	0.32	20120626	-	-	0.15	20111025
J0204+152	0.45	20120626	-	-	-	-
J0204-170	2.34	20120609	1.13	20120720	0.37	20130723
J0205+322	0.73	20120626	-	-	0.36	20111025
J020734+315158	0.07	20120626	-	-	-	-
J020936+135156	0.32	20120626	-	-	-	-
J0211-5101	1.73	20120609	1.03	20120902	0.85	20130723
J0214-6149	0.43	20120807	0.22	20120902	-	-
J0216-0223	0.12	20120804	-	-	-	-
J0216-3247	0.17	20120609	0.11	20120720	-	-
J0217+017	0.8	20120626	-	-	0.43	20120601
J0219+0121	0.28	20120626	-	-	0.14	20111016
J0222-346	0.36	20120512	0.22	20120901	-	-
J0224-5348	0.1	20120609	-	-	-	-
J0224+069	0.9	20120626	-	-	0.57	20120601
J022504+184652	0.04	20120626	-	-	-	-
J0227-3026	0.24	20120512	0.16	20120720	0.11	20120601
J0229-5403	0.11	20120609	-	-	-	-
J0231-4746	0.43	20120512	0.34	20120902	0.22	20120601
J0232+1323	0.77	20120807	-	-	-	-
J023228+262840	0.14	20120807	-	-	-	-
J0237+288	1.81	20130701	1.59	20121020	0.97	20131019
J0238+166	0.95	20130701	0.96	20121006	0.53	20131019
J0239-0235	0.32	20120804	-	-	0.34	20111025
J0239+042	0.18	20120807	-	-	-	-
J0240-231	0.14	20120512	0.05	20120720	-	-
J024042+184801	0.06	20120807	-	-	-	-
J0241-082	0.87	20120804	0.55	20120901	0.46	20111016
J024224+174308	0.2	20120807	-	-	-	-
J0243-2132	0.08	20120626	-	-	-	-
J024518+240530	0.42	20120807	-	-	-	-
J0245-4459	0.35	20120512	-	-	0.17	20120601
J0249+0620	0.13	20120804	-	-	-	-
J025207+171842	0.33	20120807	-	-	-	-
J025851+054053	0.12	20120804	-	-	-	-
J0259+0748	0.52	20120807	-	-	0.42	20111025
J030123+011838	0.2	20120804	-	-	-	-
J030441+334855	0.13	20120807	-	-	-	-
J0309+1029	1.5	20120807	-	-	0.63	20111025
J031243+013258	0.43	20120804	0.3	20120901	0.1	20111025
J0320+4131	15.29	20121129	10.21	20121020	5.94	20131019
J032759+004411	0.14	20120804	-	-	-	-
J0330-2357	0.52	20120512	0.37	20120901	0.26	20111101
J0334-401	1.0	20130701	0.98	20121006	0.42	20131019
J0337-3616	0.26	20120626	-	-	0.2	20111008
J033930-014638	2.03	20120804	1.38	20120901	0.69	20130723
J0340-213	0.46	20120626	0.36	20120901	0.32	20111101
J0349-2749	0.35	20120512	0.23	20120901	0.23	20111008
J0349-1610	0.59	20120626	0.46	20120901	0.42	20111101
J0349-2102	0.32	20120626	0.25	20120901	-	-
J0351-1153	0.18	20120626	-	-	0.07	20111101
J0352-2514	0.23	20120512	-	-	0.15	20111008
J040220-314710	0.45	20120512	0.27	20120901	-	-
J0407-3826	0.79	20120626	0.67	20120901	-	-
J040734-330329	0.19	20120626	-	-	-	-
J040906-123853	0.05	20120731	-	-	-	-
J0416-2056	0.21	20120731	0.13	20120901	-	-
J0417-1851	0.19	20120731	-	-	-	-
J0418+380	2.19	20110906	2.5	20110726	1.22	20111009
J0423-0121	3.42	20130701	3.6	20121020	1.26	20131020
J0425-3756	1.4	20120721	1.0	20120901	-	-

Continued on next page

Table A.1 – Continued from previous page

J0428+3300	0.05	20110927	-	-	-	-
J0429-3756	0.91	20120731	0.8	20120901	0.6	20120603
J043103+203719	0.19	20110927	-	-	-	-
J0433+053	1.4	20110906	1.59	20120821	0.67	20111009
J043735-295403	0.07	20120731	-	-	-	-
J0438+3005	0.26	20110927	0.12	20120902	-	-
J0440-6952	0.27	20111030	-	-	0.14	20111025
J0449+113	1.11	20110927	-	-	0.44	20120603
J0453-281	0.65	20120721	0.32	20120821	0.3	20120603
J0457-2325	1.6	20120721	1.57	20120821	1.02	20120603
J0505+049	0.79	20120804	0.34	20120821	-	-
J0507-6110	0.42	20111030	0.21	20120821	0.19	20111025
J0509+056	0.31	20120804	-	-	-	-
J0510+180	3.2	20130322	2.09	20121019	1.09	20130929
J0513-219	0.23	20120721	-	-	-	-
J051614-160312	0.21	20120721	-	-	-	-
J051910+084858	0.48	20120804	-	-	-	-
J0519-454	1.78	20130322	1.18	20121019	0.79	20131020
J0521+166	0.63	20120901	-	-	-	-
J0522-364	6.04	20130322	5.84	20121019	4.18	20131020
J0527+035	0.36	20120804	-	-	0.2	20120603
J0530-7245	0.39	20111030	0.81	20120821	0.23	20111025
J0531+1332	2.11	20120901	-	-	1.56	20120603
J0532+075	1.65	20120901	1.36	20120902	0.72	20120603
J0538-440	3.57	20130322	2.19	20121006	1.36	20131020
J0540+1434	1.24	20120901	-	-	-	-
J0540-2840	0.62	20120901	0.31	20120821	-	-
J0540-5418	0.37	20120901	0.16	20120821	-	-
J0550-5732	0.5	20120901	0.3	20120821	-	-
J0552+032	0.27	20120804	-	-	-	-
J0559-4529	0.38	20120901	0.25	20120821	-	-
J0600+2354	0.11	20120804	-	-	-	-
J0600-3937	0.51	20120901	0.28	20120821	-	-
J0601-7036	0.25	20111030	-	-	0.16	20111025
J0605+2430	0.18	20120901	-	-	-	-
J0609-2220	0.35	20120901	-	-	-	-
J0609-157	1.23	20120804	-	-	0.6	20120603
J0614+1307	0.21	20120804	-	-	-	-
J0623-6436	0.36	20111030	0.28	20120821	0.26	20111025
J0626+1440	0.08	20120804	-	-	-	-
J0629-1959	1.05	20120804	-	-	0.54	20120603
J063326-222321	0.55	20120901	-	-	-	-
J0635-2335	0.38	20120901	-	-	-	-
J0635-7516	1.23	20130705	0.67	20121006	0.33	20131020
J0642-0321	0.55	20120804	-	-	-	-
J0643+0858	0.38	20120804	-	-	-	-
J0648-3044	1.04	20120901	-	-	-	-
J0653+370	0.14	20120804	-	-	-	-
J0700+171	0.9	20120804	-	-	-	-
J0701-4634	1.28	20120901	0.67	20120821	-	-
J070231+264404	0.2	20120804	-	-	-	-
J0725+144	0.33	20120804	-	-	-	-
J0730-1141	1.22	20111111	-	-	0.47	20111113
J0739+016	0.9	20120328	-	-	-	-
J0745+101	0.25	20120328	-	-	-	-
J0745-007	0.32	20120328	-	-	-	-
J074641+273454	0.23	20120328	-	-	-	-
J0749+2400	0.52	20120328	-	-	-	-
J075000+182311	0.28	20120328	-	-	-	-
J0750+125	1.72	20130322	1.23	20121019	0.75	20131020
J0757+0957	1.08	20120328	-	-	-	-
J0802+181	0.08	20120328	-	-	-	-
J0808-0751	0.49	20120328	-	-	-	-
J0811+0147	0.37	20120328	-	-	-	-
J0831+044	1.25	20111111	-	-	0.92	20111113
J0835-5953	0.3	20111111	-	-	-	-
J0855+2007	5.23	20130705	3.08	20121006	1.65	20131020
J0909+013	1.3	20111111	-	-	0.54	20111113

Continued on next page

Table A.1 – Continued from previous page

J0915+0246	0.5	20111111	-	-	0.24	20111113
J0921-2957	0.29	20120515	-	-	-	-
J0921+0805	0.08	20111111	-	-	0.05	20111113
J0921-263	0.53	20120515	-	-	-	-
J0923-4000	0.63	20120515	-	-	-	-
J0927+390	4.36	20111111	-	-	1.73	20111113
J0928-2035	1.54	20120515	-	-	-	-
J0931-8534	0.17	20120807	-	-	-	-
J0943-083	0.07	20120515	-	-	-	-
J1002-4438	0.1	20120515	-	-	-	-
J1006-5018	0.74	20120515	-	-	0.59	20111115
J1007-0207	0.25	20120515	-	-	-	-
J1008+063	0.33	20111111	-	-	0.21	20111113
J1035-2012	0.51	20120515	-	-	-	-
J103716-293421	0.67	20130705	0.83	20121006	0.34	20131019
J1048-6217	0.44	20120125	-	-	0.24	20111028
J105830+013340	1.63	20130705	1.58	20121006	0.86	20131019
J1059-8004	1.85	20120807	-	-	0.02	20111028
J1102-6325	0.36	20111119	-	-	-	-
J1107-4449	1.43	20130705	0.75	20121006	0.49	20131019
J1112-5704	0.29	20120516	-	-	-	-
J1113-2158	0.05	20120516	-	-	-	-
J1130-1449	1.21	20111111	-	-	0.49	20120615
J1132-5819	0.29	20111205	-	-	-	-
J1146-6954	0.85	20120125	-	-	0.21	20111028
J1146-2859	0.41	20120516	-	-	-	-
J1146-3329	0.18	20120516	-	-	-	-
J114657+395840	0.82	20121203	-	-	0.39	20130417
J114702-381207	1.72	20111119	-	-	-	-
J114702-381207	1.72	20111119	-	-	-	-
J114702-381207	1.72	20111119	-	-	-	-
J1147-3812	1.72	20111119	-	-	-	-
J114702-381207	1.72	20111119	-	-	-	-
J114702-381207	1.72	20111119	-	-	-	-
J1147-6753	1.04	20120125	0.58	20111118	0.7	20111115
J1151-0024	0.31	20120326	-	-	-	-
J1153-8344	0.13	20120807	-	-	-	-
J1154-3505	0.2	20120516	-	-	-	-
J1200+2915	0.7	20120307	-	-	0.45	20111204
J121503+165456	0.48	20120326	-	-	-	-
J121546-173142	0.75	20111119	0.39	20120114	0.28	20120615
J1220+0204	0.65	20120326	-	-	0.37	20120615
J122221+041316	0.73	20120326	-	-	-	-
J1224-8313	0.24	20120807	-	-	0.07	20111028
J1225+2123	1.13	20120326	-	-	-	-
J1227-4437	0.63	20120120	-	-	-	-
J1229+020	6.63	20130705	2.95	20121006	1.91	20131019
J1230+123	2.43	20120326	-	-	-	-
J123924+073015	0.9	20120326	-	-	0.51	20120112
J1246-1617	0.36	20111119	-	-	-	-
J1246-0731	0.68	20120326	0.35	20120114	0.25	20120615
J1248-4600	0.27	20120128	0.15	20111118	-	-
J1256-057	17.69	20130705	13.07	20121006	6.93	20131019
J1304-5541	0.5	20120128	0.35	20111118	-	-
J1305-0346	0.39	20120326	-	-	-	-
J1308-6707	0.6	20120128	-	-	-	-
J1311+3234	0.23	20120802	-	-	-	-
J1316-3339	0.89	20120120	0.43	20120114	-	-
J131736+342514	0.44	20120802	-	-	-	-
J132111+221553	0.33	20120802	-	-	-	-
J1321-4342	0.43	20120120	-	-	-	-
J1326+3154	0.21	20120802	-	-	-	-
J1329-5608	2.2	20120128	0.97	20111118	-	-
J132953+315417	0.35	20120802	-	-	-	-
J1330+251	0.32	20120802	-	-	-	-
J1331+305	0.75	20120802	-	-	-	-
J1333+0201	0.82	20111119	-	-	0.44	20120702
J133739-125720	5.85	20130705	4.14	20121006	2.54	20130510

Continued on next page

Table A.1 – Continued from previous page

J134209+270936	0.22	20120802	-	-	-	-
J1342-2901	0.32	20120120	-	-	-	-
J1348+1217	0.61	20120516	-	-	0.25	20120702
J1351+3035	0.12	20120516	-	-	-	-
J1351-148	0.26	20120516	-	-	-	-
J1354-0206	0.23	20120516	-	-	-	-
J135704+191919	0.65	20120128	-	-	0.37	20120702
J135706-174402	0.07	20120513	-	-	-	-
J1357-1527	0.46	20120516	-	-	-	-
J1359+0200	0.45	20120516	-	-	0.15	20120702
J140500+041544	0.23	20120516	-	-	-	-
J1409-0752	0.54	20111119	-	-	0.31	20111206
J1410+0203	0.47	20120516	-	-	0.24	20120702
J141559+132015	0.47	20120128	-	-	0.24	20120702
J1419-3510	0.26	20120129	-	-	-	-
J1420-5155	0.22	20120128	-	-	-	-
J141958+270625	0.26	20120516	-	-	-	-
J142433-491359	0.86	20120513	-	-	-	-
J1426+1425	0.31	20120516	-	-	-	-
J1427+3625	0.33	20120307	0.16	20110613	0.15	20111204
J1428-3306	1.03	20120129	-	-	-	-
J1428-4206	7.45	20130705	3.93	20121006	4.1	20130510
J1430+1043	0.14	20111119	-	-	0.05	20111206
J1433-1802	0.24	20120516	-	-	-	-
J1433-1549	0.15	20120513	-	-	-	-
J1433-8341	0.13	20120323	-	-	-	-
J143440+195215	0.2	20120516	-	-	-	-
J143809-220449	0.3	20120513	-	-	-	-
J143956-153143	0.2	20120516	-	-	-	-
J1446-1629	0.4	20120516	-	-	-	-
J1447+1721	0.24	20120128	-	-	0.1	20111206
J144850+040215	0.17	20120516	-	-	-	-
J145031+091012	0.21	20120516	-	-	-	-
J145427-374734	1.89	20120513	-	-	0.37	20110923
J145432-401228	0.21	20120513	-	-	-	-
J1457-3539	1.33	20120513	-	-	-	-
J145859+041600	0.21	20120516	-	-	0.15	20120120
J150424+102943	0.84	20120128	-	-	0.29	20120702
J1505+0327	0.22	20120516	-	-	-	-
J1509-4953	1.24	20120513	-	-	0.21	20111016
J1511-0543	0.44	20120516	-	-	-	-
J151639+001509	1.04	20120802	-	-	0.94	20120120
J151743-242216	1.7	20130705	1.29	20121006	0.82	20130510
J152122+042041	0.13	20120802	-	-	-	-
J1523-2730	0.35	20120513	-	-	-	-
J1527-1351	0.08	20120513	-	-	-	-
J1535-3526	0.27	20120129	-	-	-	-
J154048+144739	0.64	20120802	-	-	0.32	20120604
J154301-075705	0.1	20120802	-	-	-	-
J1546+0026	0.14	20120802	-	-	-	-
J155035+052702	1.01	20130705	0.59	20121006	0.27	20131001
J1554+1257	0.34	20120802	-	-	-	-
J1554-2705	0.14	20120802	-	-	-	-
J155543+111127	0.16	20120802	-	-	-	-
J1558-0002	0.24	20120513	-	-	-	-
J1600-2443	0.07	20120513	-	-	-	-
J1600-5811	0.39	20120513	-	-	-	-
J160338+155357	0.06	20120802	-	-	-	-
J160342+110547	0.26	20120802	-	-	-	-
J1608-3331	0.08	20120513	-	-	-	-
J1609+1029	0.23	20120802	-	-	-	-
J1617-5848	1.36	20130702	1.17	20121006	0.44	20131001
J1618-7717	0.97	20120323	-	-	-	-
J1618+0247	0.14	20120802	-	-	-	-
J1619+2248	0.21	20120802	-	-	-	-
J1624-3517	0.1	20120127	-	-	-	-
J1626-2528	1.32	20120513	-	-	1.1	20120602
J1635+3808	4.3	20120902	-	-	-	-

Continued on next page

Table A.1 – Continued from previous page

J1637-4102	0.31	20120127	-	-	-	-
J1640+3947	0.37	20120802	-	-	-	-
J164047+122013	0.04	20120513	-	-	-	-
J1641+2257	0.11	20120902	-	-	-	-
J1643+2523	0.22	20120902	-	-	-	-
J1642+398	2.9	20130702	1.49	20110613	1.16	20130702
J164733+270607	0.13	20120902	-	-	-	-
J1648+2225	0.18	20120902	-	-	-	-
J1649-3302	0.19	20120127	-	-	-	-
J1650-5045	0.91	20120129	-	-	-	-
J1651-2944	1.07	20120322	-	-	-	-
J165102+012926	0.22	20120513	-	-	-	-
J1653+3108	0.24	20120902	-	-	-	-
J165809+074125	1.14	20120802	-	-	0.7	20120602
J165832+051515	0.11	20120407	-	-	-	-
J165842-073921	0.04	20120513	-	-	-	-
J165924+262934	0.27	20120902	-	-	-	-
J1701-5621	0.37	20120802	-	-	-	-
J1704-6213	1.01	20120323	-	-	-	-
J1708+0149	0.24	20120407	-	-	-	-
J170745+133117	0.35	20120407	-	-	-	-
J170753+184642	0.07	20120902	-	-	-	-
J1709-3525	0.24	20120322	-	-	-	-
J1714-2659	0.26	20120513	-	-	-	-
J171610+215203	0.21	20120902	-	-	-	-
J1718-3342	1.21	20120127	-	-	0.57	20110923
J1718-3949	0.1	20120513	-	-	-	-
J171909+065815	0.14	20120407	-	-	-	-
J171913+174506	0.68	20120407	-	-	-	-
J1720+0817	0.03	20120513	-	-	-	-
J1720-3553	0.83	20120127	-	-	0.26	20120606
J172244+101323	0.12	20120513	-	-	-	-
J1724-6501	0.59	20120323	-	-	-	-
J172807+121541	0.8	20120407	-	-	-	-
J1733-130	2.32	20130702	1.66	20121006	0.92	20131001
J1733-3723	0.75	20120127	-	-	-	-
J1734+3858	1.05	20120902	-	-	-	-
J173458+092658	0.08	20120513	-	-	-	-
J1736+3617	0.34	20120902	-	-	-	-
J1737+0621	0.18	20120407	-	-	-	-
J174005+221058	0.25	20120407	-	-	-	-
J1743-3058	0.03	20120513	-	-	-	-
J174358+193509	0.1	20120902	-	-	-	-
J1744-3117	0.47	20120322	-	-	-	-
J1744-5145	0.15	20120322	-	-	-	-
J174504+225249	0.1	20120902	-	-	-	-
J174528-075306	0.85	20120406	-	-	-	-
J174534+171957	0.15	20120407	-	-	-	-
J175132+093858	2.7	20130702	2.25	20121006	1.17	20131001
J175143+292054	0.14	20120407	-	-	-	-
J175246+173417	0.22	20120902	-	-	-	-
J1754+2848	0.46	20120406	-	-	-	-
J175511+335057	0.05	20120902	-	-	-	-
J1755-2232	0.17	20120322	-	-	-	-
J1757+1535	0.27	20120406	-	-	-	-
J1800+3849	0.16	20120124	-	-	-	-
J180024+384834	0.16	20120124	0.06	20110611	-	-
J1803-3940	1.3	20120322	-	-	-	-
J1803-6508	0.48	20120322	-	-	-	-
J180333+093412	0.06	20120406	-	-	-	-
J180356+034100	0.16	20120513	-	-	-	-
J180415+010126	0.15	20120406	-	-	-	-
J1808-2506	0.09	20120513	-	-	-	-
J1808-6414	0.19	20120323	-	-	-	-
J1810-4553	1.26	20120322	-	-	-	-
J181143+170500	0.41	20120902	-	-	-	-
J1813-0648	0.06	20120513	-	-	-	-
J181333+061531	0.17	20120406	-	-	-	-

Continued on next page

Table A.1 – Continued from previous page

J1818-1109	0.04	20120513	-	-	-	-
J1819-6345	0.34	20120323	-	-	0.14	20120606
J1821-2528	0.44	20120327	-	-	0.15	20120606
J182210+160026	0.49	20120406	-	-	-	-
J1824+1044	0.24	20120513	-	-	-	-
J1825+0120	0.13	20120406	-	-	-	-
J1826-1719	0.07	20120513	-	-	-	-
J1826-0738	0.1	20120513	-	-	-	-
J1830+0619	0.56	20120406	-	-	0.36	20110917
J1832-2040	0.31	20120327	-	-	0.18	20120606
J1832-1035	0.34	20120406	-	-	-	-
J1833+0732	0.18	20120902	-	-	-	-
J1833+1358	0.21	20120406	-	-	-	-
J183249+283336	0.23	20120902	-	-	-	-
J1834-0301	0.06	20120513	-	-	-	-
J1834-5857	0.27	20120323	-	-	-	-
J1837-7109	0.35	20120323	-	-	-	-
J1839+0404	0.19	20120406	-	-	-	-
J184821+321903	0.58	20120902	-	-	0.26	20110917
J1852+0036	0.5	20120406	-	-	-	-
J1857+0610	0.11	20120406	-	-	-	-
J1907+0127	0.18	20120406	-	-	-	-
J1912-1504	0.15	20120406	0.07	20120626	-	-
J192451-291428	4.77	20130923	3.97	20121022	2.36	20131021
J1929+0508	0.13	20120406	0.05	20120627	-	-
J1931+1533	0.23	20120406	-	-	-	-
J1931+2244	0.24	20120406	-	-	-	-
J1935+2032	0.62	20120406	-	-	-	-
J1939+0448	0.17	20120406	-	-	-	-
J193926-152551	0.41	20120406	0.19	20120626	-	-
J1946-3112	0.26	20120327	0.09	20120627	0.08	20120606
J1953+2527	0.27	20120406	-	-	-	-
J1955+1358	0.37	20120406	0.28	20120627	-	-
J1957+2821	0.13	20120406	-	-	-	-
J1957-3226	0.39	20120327	0.19	20120627	-	-
J2003+1501	0.26	20120406	0.17	20120627	-	-
J2005-1822	0.33	20120406	0.16	20120626	-	-
J200556-372350	0.22	20120327	-	-	-	-
J200711+063648	0.08	20120324	-	-	-	-
J2008+4030	1.16	20120407	-	-	-	-
J2009-4850	0.46	20120327	0.32	20120627	-	-
J201115-064410	0.03	20120324	-	-	-	-
J201115-154641	0.99	20120406	0.43	20120626	-	-
J2015+3411	0.07	20120407	-	-	-	-
J201614+163217	0.22	20120324	-	-	-	-
J2021+2319	0.11	20120406	-	-	-	-
J2023+3153	0.79	20120406	-	-	0.51	20110917
J202422+002751	0.08	20120324	-	-	-	-
J2025+2736	0.13	20120406	-	-	-	-
J2025+1718	0.13	20120324	-	-	-	-
J202509+031646	0.24	20120324	-	-	-	-
J2025+3343	2.25	20130821	1.05	20110724	0.88	20131002
J2025-0735	1.68	20120324	0.99	20120720	-	-
J203154+121929	0.84	20120324	0.36	20120720	0.36	20120602
J2033+4040	1.23	20120407	-	-	-	-
J203522+105554	0.17	20120324	0.32	20120626	0.19	20111014
J2035-6846	0.58	20120323	0.24	20120623	-	-
J2036-6602	0.09	20120323	-	-	-	-
J2047-026	0.07	20120406	-	-	-	-
J204719-163904	0.03	20120406	-	-	-	-
J204945+100303	0.33	20120406	0.21	20120720	0.11	20111014
J2050+0408	0.31	20120324	0.21	20120720	-	-
J205134+174324	0.57	20120406	0.31	20120720	0.31	20120602
J2056-4715	1.03	20130923	0.99	20121022	0.54	20131021
J2058-3734	0.28	20120408	0.26	20120112	-	-
J2101-2933	0.42	20120324	0.36	20120112	-	-
J210138+034107	0.94	20120406	0.35	20120720	-	-
J2109+1430	0.41	20120406	0.14	20120720	0.15	20120602

Continued on next page

Table A.1 – Continued from previous page

J2110+3533	0.5	20120804	-	-	-	-
J2110-4110	0.29	20120408	0.21	20120112	-	-
J211457+283247	0.29	20120801	-	-	-	-
J2115+2934	0.39	20120804	-	-	-	-
J211721+050246	0.15	20120406	-	-	-	-
J2121-3703	0.12	20111023	0.06	20120627	-	-
J212313+100751	0.19	20120801	-	-	-	-
J212344+053534	1.03	20120406	0.77	20120720	0.44	20111014
J2127-4606	0.51	20120902	0.24	20120627	-	-
J2130-0927	0.31	20120324	0.23	20120623	-	-
J2139-2440	0.19	20120324	0.09	20120627	-	-
J2139+1424	0.56	20120804	0.19	20120623	-	-
J2143-2445	0.23	20120324	-	-	-	-
J2143-0438	0.15	20120324	-	-	-	-
J214518+111542	0.16	20120801	-	-	-	-
J2147+0930	0.31	20120804	0.2	20120623	-	-
J214805+065743	2.42	20130923	1.01	20121006	0.9	20131021
J214935+075622	0.09	20120801	-	-	-	-
J2151-2742	0.54	20120324	0.38	20120627	-	-
J2152+0709	0.32	20120324	0.15	20120623	-	-
J2152-3028	0.7	20111023	0.42	20120902	-	-
J215225+173414	0.37	20120324	0.25	20120623	-	-
J215440+172753	0.12	20120801	-	-	-	-
J215506+225026	0.13	20120324	-	-	-	-
J2157-6941	1.3	20120124	0.88	20110724	0.42	20130723
J2157+1014	0.16	20120324	-	-	-	-
J215727+312654	0.61	20120801	-	-	-	-
J215852-301328	0.25	20120324	-	-	-	-
J220013+213750	0.11	20120902	-	-	-	-
J2201-5520	0.34	20111023	0.13	20120902	-	-
J2202+422	8.91	20111031	2.72	20110724	-	-
J2203-2335	0.23	20120324	-	-	-	-
J220315+314538	1.25	20111031	0.76	20110724	-	-
J220326+172542	0.55	20120804	0.37	20120623	-	-
J220420+363226	0.05	20120801	-	-	-	-
J220610-183534	0.57	20111025	-	-	-	-
J2210+3556	0.13	20120801	-	-	-	-
J2211-1328	0.28	20120324	0.17	20120622	-	-
J221205+235531	0.42	20120804	0.23	20120622	-	-
J221207+330842	0.02	20120902	-	-	-	-
J2213+0153	0.05	20120801	-	-	-	-
J221238+275944	0.09	20120902	-	-	-	-
J221302-252932	0.28	20120324	0.18	20120902	-	-
J2216+3518	0.24	20120902	-	-	-	-
J221643+310245	0.06	20120902	-	-	-	-
J2217+2422	0.51	20120804	0.38	20120622	-	-
J221851-033540	0.57	20120408	0.2	20120622	-	-
J2219+1807	0.16	20120902	0.09	20120622	-	-
J2223-3137	0.36	20120408	0.21	20120902	-	-
J2226+2118	0.31	20120902	0.12	20120622	-	-
J2225-049	1.64	20111031	1.08	20110724	0.42	20130723
J222645+005159	0.28	20120324	0.16	20120622	-	-
J2229-6911	0.27	20120408	-	-	-	-
J222940-083254	2.2	20111025	0.67	20120622	-	-
J2230-1326	0.24	20120408	-	-	-	-
J2233+1144	2.24	20130923	4.89	20121022	1.18	20131021
J223513-483557	0.9	20111023	0.44	20120902	-	-
J223620+282856	2.18	20120902	-	-	-	-
J223813+274941	0.14	20120902	-	-	-	-
J2239-5701	0.79	20111023	0.32	20120623	-	-
J224326-254429	0.38	20120408	-	-	-	-
J2246-5607	0.28	20111023	0.12	20120623	-	-
J224617-120653	0.01	20111025	-	-	-	-
J224704-365755	0.32	20120408	-	-	-	-
J2248+0311	0.17	20120324	-	-	-	-
J2249-3236	0.88	20120408	0.44	20120902	-	-
J224900+210719	0.2	20120324	-	-	-	-
J2250-2806	0.52	20120408	0.37	20120902	-	-

Continued on next page

Table A.1 – Continued from previous page

J225307+194231	0.22	20120324	-	-	-	-
J2253+161	3.25	20120324	2.47	20111126	4.6	20130723
J2254+2445	0.16	20120527	-	-	-	-
J2257-2012	0.69	20120408	-	-	-	-
J225716+074314	0.52	20120527	0.4	20120902	-	-
J225717+024311	0.09	20120324	-	-	-	-
J225717+024311	0.09	20120324	-	-	-	-
J225805-275823	1.32	20130923	3.25	20121020	0.58	20131021
J2301-0158	0.58	20120324	0.28	20120902	-	-
J2303-1841	0.42	20111025	-	-	-	-
J2307+3231	0.12	20120527	-	-	-	-
J2311+3425	0.45	20120527	-	-	-	-
J231448-313835	0.17	20120530	-	-	-	-
J2315-5018	0.91	20120408	0.45	20120623	-	-
J232045+051358	0.52	20120527	0.5	20120902	0.18	20111013
J232155+320409	0.33	20120527	-	-	-	-
J2322+2733	0.41	20120527	-	-	-	-
J2329-4730	1.12	20111023	0.4	20120623	-	-
J2332-1557	0.44	20120530	0.2	20120902	-	-
J2334+0736	0.72	20120512	0.56	20120902	0.32	20111013
J2335-5251	0.21	20111023	0.1	20120902	-	-
J2340-3310	0.13	20120408	0.05	20120623	-	-
J234312+233926	0.13	20120527	-	-	-	-
J234511-155507	1.09	20111025	0.92	20120902	-	-
J2346+095	0.25	20120512	-	-	-	-
J234803-163113	1.63	20111025	1.12	20120902	-	-
J2349+0535	0.2	20120512	-	-	-	-
J2355-1513	0.32	20111025	-	-	-	-
J235732-112536	0.23	20120530	0.11	20120902	-	-
J2358-5311	1.04	20130923	0.78	20121020	0.45	20131021
J235810-102004	0.67	20111025	0.32	20120902	-	-
J2359+1955	0.09	20120512	-	-	-	-
J2359-3133	0.24	20120530	-	-	-	-